Free Radical Biology and Medicine 139 (2019) 55–69

Contents lists available at ScienceDirect

Free Radical Biology and Medicine

journal homepage: www.elsevier.com/locate/freeradbiomed

Original article

Staphylococcus aureus responds to allicin by global *S*-thioallylation – Role of the Brx/BSH/YpdA pathway and the disulfide reductase MerA to overcome allicin stress

Vu Van Loi[a], Nguyen Thi Thu Huyen[a,1], Tobias Busche[a,b], Quach Ngoc Tung[a], Martin Clemens Horst Gruhlke[c], Jörn Kalinowski[b], Jörg Bernhardt[a,d], Alan John Slusarenko[c], Haike Antelmann[a,*]

[a] Freie Universität Berlin, Institute for Biology-Microbiology, D-14195, Berlin, Germany
[b] Center for Biotechnology, Bielefeld University, D-33594, Bielefeld, Germany
[c] Department of Plant Physiology, RWTH Aachen University, D-52056, Aachen, Germany
[d] Institute for Microbiology, University of Greifswald, D-17489, Greifswald, Germany

ARTICLE INFO

Keywords:
Staphylococcus aureus
Allicin
Bacillithiol
S-thioallylation
MerA
BrxAB
YpdA

ABSTRACT

The prevalence of methicillin-resitant *Staphylococcus aureus* (MRSA) in hospitals and the community poses an increasing health burden, which requires the discovery of alternative antimicrobials. Allicin (diallyl thiosulfinate) from garlic exhibits broad-spectrum antimicrobial activity against many multidrug resistant bacteria. The thiol-reactive mode of action of allicin involves its *S*-thioallylations of low molecular weight (LMW) thiols and protein thiols. To investigate the mode of action and stress response caused by allicin in *S. aureus*, we analyzed the transcriptome signature, the targets for *S*-thioallylation in the proteome and the changes in the bacillithiol (BSH) redox potential (E_{BSH}) under allicin stress. Allicin caused a strong thiol-specific oxidative and sulfur stress response and protein damage as revealed by the induction of the PerR, HypR, QsrR, MhqR, CstR, CtsR, HrcA and CymR regulons in the RNA-seq transcriptome. Allicin also interfered with metal and cell wall homeostasis and caused induction of the Zur, CsoR and GraRS regulons. Brx-roGFP2 biosensor measurements revealed a strongly increased E_{BSH} under allicin stress. In the proteome, 57 proteins were identified with *S*-thioallylations under allicin treatment, including translation factors (EF-Tu, EF-Ts), metabolic and redox enzymes (AldA, GuaB, Tpx, KatA, BrxA, MsrB) as well as redox-sensitive MarR/SarA-family regulators (MgrA, SarA, SarH1, SarS). Phenotype and biochemical analyses revealed that BSH and the HypR-controlled disulfide reductase MerA are involved in allicin detoxification in *S. aureus*. The reversal of protein *S*-thioallylation was catalyzed by the Brx/BSH/YpdA pathway. Finally, the BSSB reductase YpdA was shown to use *S*-allylmercaptobacillithiol (BSSA) as substrate to regenerate BSH in *S. aureus*. In conclusion, allicin results in an oxidative shift of E_{BSH} and protein *S*-thioallylation, which can be reversed by YpdA and the Brx/BSH/YpdA electron pathways in *S. aureus* to regenerate thiol homeostasis.

1. Introduction

Staphylococcus aureus is an opportunistic human pathogen that causes many diseases, ranging from local skin abscesses to life-threatening systemic and chronic infections, including septicemia, endocarditis, pneumonia and osteomyelitis [1–3]. *S. aureus* isolates are the leading cause of nosocomial infections, and are often resistant to multiple antibiotics, including methicillin-resistant *S. aureus* (MRSA) [4]. Due to the prevalence of MRSA infections, *S. aureus* belongs to the most dangerous ESKAPE pathogens [5]. The increasing problem of antimicrobial resistance demands the design of alternative antimicrobials and discovery of natural compounds with antibiotic properties, which do not cause resistance development.

Thiol-reactive natural compounds, such as the garlic-derived diallyl thiosulfinate allicin have long been used as broad-spectrum antimicrobials to threat bacterial infections [6,7]. Allicin is produced in garlic plants (*Allium sativum*) upon wounding from the odor-less precursor alliin. The cysteine-*S*-lyase alliinase is released from the vacuole

* Corresponding author. Institute of Biology-Microbiology, Freie Universität Berlin, Königin-Luise-Strasse 12-16, D-14195, Berlin, Germany.
E-mail address: haike.antelmann@fu-berlin.de (H. Antelmann).
[1] Current address: Ho Chi Minh University of Food Industry, Faculty of Biotechnology, Ho Chi Minh City, Vietnam.

https://doi.org/10.1016/j.freeradbiomed.2019.05.018
Received 27 March 2019; Received in revised form 8 May 2019; Accepted 15 May 2019
Available online 20 May 2019

into the cytosol upon garlic tissue damage, generating allyl sulfenic acid and dehydroalanine from alliin [8,9]. Two allyl sulfenic acid molecules condense to form the thiol-reactive diallyl thiosulfonate (allicin), which gives garlic its characteristic odor [10]. Allicin can further decompose upon heating into diallyl disulfides and diallyl polysulfanes with up to seven sequential sulfur atoms, which are also thiol-reactive [11,12]. Allicin and diallyl polysulfanes showed broad-spectrum antimicrobial activity against various Gram-positive and Gram-negative bacteria, including multi-resistant *S. aureus*, *Streptococcus pneumoniae, Pseudomonas aeruginosa, Helicobacter pylori, Escherichia coli, Bacillus subtilis* and *Klebsiella pneumoniae* as well as fungi, such as *Candia albicans* and parasites [10–16]. Due to its volatile nature, allicin can be applied via the pulmonary route as a vapor by inhalation, which makes it attractive for antimicrobial treatment of respiratory pathogens to combat pneumonia infections [13]. Indeed a historical precedent for this is known from the pre-streptomycin era for the treatment of tuberculosis infections caused by *Mycobacterium tuberculosis* [17].

The antimicrobial mode of action of allicin has been studied in detail in *E. coli* previously [14]. Allicin has been shown to cause depletion of the low molecular weight (LMW) thiol glutathione (GSH), by a thiol-disulfide exchange reaction, leading to *S*-allylmercaptoglutathione (GSSA). In *E.coli* and human cells, significant protein *S*-thioallylation has been demonstrated after allicin exposure [14,15,18,19]. In the Gram-positive bacterium *B. subtilis*, depletion of several LMW thiols, including bacillithiol (BSH), cysteine and coenzyme A by garlic derived diallyl polysulfanes has been recently reported using thiol metabolomics [16]. As a volatile compound, allicin can easily penetrate the cellular phospholipid membrane, which contributes to its antimicrobial mode of action. Moreover, allicin can cause pore formation in biological membranes and artificial lipid bilayers, facilitating the uptake and action of other antibiotics [20,21]. This ability of allicin to pass membranes has inspired pharmacists to design *N*-thiolated fluoroquinolone and dipyridyl antibiotics [22,23]. These thiolated antibiotics exhibited enhanced activity against MRSA and other ESKAPE pathogens due to disulfide formation with LMW thiols, generation of reactive oxygen species (ROS) and increased penetration of bacterial membranes. Thus, allicin's major antimicrobial mode of action is mainly attributed to the *S*-thioallylation of LMW thiols and protein thiols, leading to enzyme inhibition and cell death [14,15,19]. Several enzymes were inhibited by *S*-thioallylation under allicin stress *in vitro*, such as the cysteine protease papain, alcohol dehydrogenases, enolase and isocitrate lyase [14,15,18]. We have recently identified 332 proteins with *S*-thioallylations after allicin treatment in human Jurkat cells [18]. The major allicin targets were abundant cytoskeletal proteins, such as actin, tubulin, cofilin, filamin and plastin-2. In addition, heat shock chaperones, glycolytic enzymes and translation factors were modified by allicin in human Jurkat cells. In *E. coli*, allicin was further shown to cause a heat shock and oxidative stress response [14]. Allicin caused protein aggregation resulting in stabilization of the RpoH heat shock sigma factor, which controls the heat shock response [14]. Additionally, a recent study revealed that allicin leads to fragmentation of the peptidoglycan in *S. aureus*, which is proposed to be caused by *S*-thioallylation of cell wall synthesis and hydrolytic enzymes [24]. However, the detailed mode of action of allicin and the targets for *S*-thioallylation have not been studied in multi-resistant *S. aureus* isolates.

S. aureus utilizes BSH as major LMW thiol, which functions as defense mechanism against ROS, thiol-reactive compounds, antibiotics and enhances intracellular survival inside macrophages during infections [25–28]. Under HOCl stress, BSH forms mixed disulfides with proteins, termed as protein *S*-bacillithiolation, which can function in thiol-protection and redox regulation of proteins [29–31]. In addition, *S. aureus* encodes many redox-sensitive transcriptional regulators, such as the MarR-type regulators SarA, MgrA and SarZ, the Rrf2-family regulater HypR and the PerR repressor, which control antioxidant enzymes and thiol-disulfide reductases, [28,32–37]. HypR was characterized as disulfide stress-specific repressor controlling the NADPH-dependent flavin disulfide reductase MerA as defense mechanisms against HOCl, diamide and AGXX® stress [38,39]. MerA was also shown to provide protection under macrophage infections [38]. HypR senses and responds to HOCl stress by intersubunit disulfide formation, resulting in inactivation of its repressor activity and derepression of the *hypR-merA* operon [38].

Here, we used RNA-seq transcriptomics, proteomics and redox biosensor measurements to study the thiol-reactive mode of action of allicin and the targets for *S*-thioallylation in *S. aureus* USA300. We further used growth and survival assays as well as biochemical assays to reveal functions of BSH and the disulfide reductase MerA in allicin detoxification and reduction of *S*-thioallylations by the BrxAB/BSH/YpdA-pathway and the bacillithiol disulfide (BSSB) reductase YpdA in *S. aureus*. Together our data revealed an oxidative shift in E_{BSH} and extensive protein *S*-thioallylation that can be reversed by YpdA and the Brx/BSH/YpdA electron pathway to regenerate E_{BSH} and protein thiols in *S. aureus*.

2. Materials and methods

2.1. Bacterial strains, growth and survival assays

Bacterial strains are listed in Table S1. *S. aureus* strains were cultivated either in LB, RPMI or Belitsky minimal medium as described [38,40]. For genetic manipulation and cloning, *E. coli* strains were grown in LB medium. Growth and survival phenotypes analyses under allicin stress were performed with *S. aureus* COL and USA300 wild types, the *S. aureus* USA300 Δ*bshA* mutant [27], the *S. aureus* COL Δ*bshA,* Δ*merA,* Δ*ypdA,* Δ*brxAB* mutants and the *merA, ypdA, brxA* and *brxB* complemented strains as described [38]. Construction of the *ypdA*, *brxAB* mutants and *ypdA, brxA* and *brxB* complemented strains is described previously [41]. The *S. aureus* strains were grown in RPMI medium and treated with 100–300 μM allicin as described [31]. Survival assays were conducted by spotting 10 μl of serial dilutions after exposure to 200–300 μM allicin for 2 and 3 h onto LB agar plates, which were incubated overnight at 37 °C for visualization of colony forming units (CFU). Allicin was synthetized by oxidation of 3-[prop-2-en-1-yl) disulfanyl] prop-1-ene (diallyl disulfide) with peracetic acid as described previously [42].

2.2. Identification of S-thioallylated proteins using LTQ-Orbitrap mass spectrometry

S. aureus USA300 was grown in LB until an optical density at 540 nm (OD_{540}) of 2, transferred to Belitsky minimal medium and exposed to 300 μM allicin for 30 min for identification of *S*-thioallylated proteins as described [18,29]. NEM-alkylated protein extracts were prepared and used for tryptic in-gel-digestion and LTQ Orbitrap Velos mass spectrometry as described [29]. *S*-thioallylated proteins were identified by searching all tandem mass spectrometry (MS/MS) spectra against the *S. aureus* USA300 target–decoy protein sequence database extracted from UniprotKB release 12.7 (UniProt Consortium, Nucleic acids research 2007, 35, D193-197) using Sorcerer™-SEQUEST® (Sequest v. 2.7 rev.11, Thermo Electron, including Scaffold 4.0; Proteome Software, Inc., Portland, OR). The SEQUEST search was carried out with the previously used parameters [29], including a parent ion mass tolerance of 10 ppm and a fragment ion mass tolerance of 1.00 Da. Up to two tryptic mis-cleavages were allowed. Methionine oxidation (Met +15.994915 Da), cysteine alkylation by N-ethylmaleimide (Cys +125.04767 Da) and cysteine *S*-thioallylation by allicin (Cys +72.00337 Da for $C_3H_5S_1$) were set as variable modifications. The mass spectrometry data have been deposited to the ProteomeXchange Consortium via the PRIDE partner repository [43,44] with the dataset identifier PXD010338.

2.3. Cloning, expression and purification of His-tagged MerA, MerAC43S, YpdA, YpdAC14A, GapDH, BrxA and BrxB proteins in E. coli

The *merA* gene (SACOL0640) was amplified from chromosomal DNA of *S. aureus* COL by PCR using primers pET-merA-for-NheI and pET-merA-rev-BamHI (Table S3), digested with *Nhe*I and *Bam*HI and inserted into plasmid pET11b (Novagen), that was digested using the same restriction enzymes to generate plasmid pET11b-*merA*. The pET11b plasmids for overexpression of the His-tagged proteins GapDH, BrxA (SACOL1464), YpdA and YpdAC14A in *E. coli* were constructed previously [31,41]. The pET11b-*merAC43S* mutant plasmid was generated using PCR mutagenesis to replace the active site Cys43 by serine. In brief, two first-round PCR reactions were performed with primers pET-merA-for-NheI and pET-merAC43S-f1-rev as well as primers pET-merAC43S-f2-for and pET-merA-rev-BamHI using *S. aureus* COL DNA as template (Table S3). The PCR products were fused by overlap extension PCR, digested with *Nhe*I and *Bam*HI and cloned into the same sites into pET11b to generate plasmid pET11b-*merAC43S*.

For expression of His-tagged proteins (GapDH, BrxA, YpdA, YpdAC14A, MerA, MerAC43S), *E. coli* BL21(DE3) *plysS* strains carrying pET11b plasmids with the cloned genes (Table S2) were cultivated in 1 l LB medium until an OD_{600} of 0.6 followed by addition of 0.7–1 mM IPTG (isopropyl-β-D-thiogalactopyranoside) for 16 h at 25 °C. His-tagged proteins were purified using His Trap™ HP Ni-NTA columns (5 ml; GE Healthcare, Chalfont St Giles, UK) and the ÄKTA purifier liquid chromatography system (GE Healthcare) as described [38].

2.4. RNA-seq transcriptome analysis and bioinformatics

S. aureus USA300 was cultivated in Belitsky minimal medium and harvested before (control) and 30 min after exposure to 300 µM allicin stress as described [38]. RNA isolation, library preparation, next generation cDNA sequencing and read assembly were carried out as described previously [38]. Differential gene expression analysis of 3 biological replicates was performed using DESeq2 [45] with ReadXplorer v2.2 [46] as described [38] using an adjusted p-value cut-off of $P \leq 0.05$ and a signal intensity ratio (M-value) cut-off of $\geq +0.6$ or ≤ -0.6 (fold-change of ± 1.5). The transcriptome sequencing raw files were deposited into the ArrayExpress database (www.ebi.ac.uk/arrayexpress) under accession number E-MTAB-5667.

2.5. Construction of the Voronoi allicin transcriptome treemap

For construction of the allicin transcriptome treemap, the Paver software (DECODON GmbH, Greifswald, Germany) was applied [47]. The treemap visualizes the log2-fold changes (M-values) of the most interesting allicin-induced redox regulons using a red-blue colour gradient. Regulons are indicated with larger white labels, genes and operons are shown with smaller labels. The cell sizes are defined as absolute log2-fold changes of expression levels under allicin treatment relative to the control.

2.6. Northern blot experiments

For Northern blot analysis, RNA was isolated from *S. aureus* USA300 and *B. subtilis* strains after treatment with 100–300 µM allicin for 15 or 30 min according to previous methods description [48]. Hybridizations were performed using the digoxigenin-labelled antisense RNA probes specific for the *S. aureus* USA300 genes *azoR1 (USA300HOU_0360), ohr (USA300HOU_0835), katA (USA300HOU_1277)* and *cysK (USA300HOU_0507)* as well as paralogous *B. subtilis* genes *azoR1, ohrA, katA* and *cysK*. The RNA probes for the *S. aureus* genes were synthesized *in vitro* using T7 RNA polymerase and the gene-specific primers as listed in Table S3 as described [48]. The RNA probes specific for the *B. subtilis* genes *azoR1, ohrA, katA* and *cysK* were generated previously [49–51].

2.7. Measurement of the BSH redox potential (E_{BSH}) in S. aureus COL using the Brx-roGFP2 biosensor

S. aureus COL with the Brx-roGFP2 biosensor was treated with 5–100 µM allicin to monitor the changes in E_{BSH} as measured by its oxidation degree (OxD) [40]. For allicin injection into microplate wells, biosensor cells were grown overnight in LB with 1% xylose, harvested and transferred to Belitsky minimal medium (BMM). Cells were adjusted to an OD_{500} of 2 and distributed into the microplate wells to start injection of 5–100 µM allicin and fluorescence measurements. For OxD measurements after different times of allicin stress and DTT reduction, *S. aureus* COL Brx-roGFP2 cells were grown in shake flasks in LB to an OD_{540} of 2, transferred to BMM and exposed to 150 µM allicin. Cells were harvested before and after different times of 150 µM allicin stress, blocked with 10 mM NEM and transferred to microplate wells. Brx-roGFP2 biosensor fluorescence emission was measured at 510 nm after excitation at 405 and 488 nm using the CLARIOstar microplate reader (BMG Labtech). Samples for fully reduced and oxidized controls were treated for 10 min with 10 mM DTT and 5 mM diamide, respectively.

The OxD of the Brx-roGFP2 biosensor was determined for each sample and normalized to fully reduced (DTT-treated) and oxidized (diamide-treated) controls as described [40] based to the following equation (1):

$$OxD = \frac{I405_{sample} \times I488_{red} - I405_{red} \times I488_{sample}}{I405_{sample} \times I488_{red} - I405_{sample} \times I488_{ox} + I405_{ox} \times I488_{sample} - I405_{red} \times I488_{sample}} \quad (1)$$

The values of $I405_{sample}$ and $I488_{sample}$ are the observed fluorescence excitation intensities at 405 and 488 nm, respectively. The values of $I405_{red}$, $I488_{red}$, $I405_{ox}$ and $I488_{ox}$ represent the fluorescence intensities of fully reduced and oxidized controls, respectively.

Based on the OxD and $E^{o'}_{roGFP2}$ = - 280 mV [52], the BSH redox potential can be calculated according to the Nernst equation (2):

$$E_{BSH} = E_{roGFP2} = E^{o'}_{roGFP2} - \left(\frac{RT}{2F}\right) * \ln\left(\frac{1-OxD}{OxD}\right) \quad (2)$$

2.8. Biochemical assays for NADPH-dependent allicin detoxification by MerA, reduction of BSSA by YpdA and recovery of S-thioallylated GapDH using the BrxA/BSH/YpdA electron pathway in vitro

The purified BrxA, GapDH, YpdA and YpdAC14A proteins were pre-reduced with 10 mM DTT, followed by DTT removal with Micro Biospin 6 columns (Biorad) before the activity assays. MerA and MerAC43S proteins were incubated for 30 min with NADPH for their reduction. The NADPH-dependent reductions of allicin and BSSA by MerA, MerAC43S, YpdA or YpdAC14A proteins were analyzed by the absorbance change at 340 nm to monitor NADPH consumption using the Clariostar microplate reader. For the allicin reduction assay, 12.5 µM of purified MerA, MerAC43S, YpdA and YpdAC14A proteins were incubated with 125–250 µM allicin and 500 µM NADPH in 20 mM Tris, 1.25 mM EDTA, pH 8.0 to monitor NADPH consumption. BSSA was generated by reaction of 40 or 125 µM BSH and 40 or 125 µM allicin, respectively for 30 min. BSSA was used as substrate for reduction by YpdA or MerA as follows. About 12.5 µM of purified MerA or MerAC43S proteins were incubated with 500 µM NADPH in 20 mM Tris, 1.25 mM EDTA, pH 8.0 for 30 min, followed by addition of 125 µM BSSA, while pre-reduced YpdA or YpdAC14A proteins were added to 40 µM BSSA and 500 µM NADPH to start the reaction. NADPH consumption was monitored as absorbance decrease at 340 nm. To measure reduction of *S*-thioallylated GapDH by the BrxA/BSH/YpdA electron pathway, GapDH (40 µM) was *S*-thioallylated with 0.75 mM allicin at 37 °C for 10 min, followed by removal of excess allicin with Micro Biospin 6 columns. Before the reaction of *S*-thioallylated GapDH with the BrxA/

BSH/YpdA electron pathway, 2.5 μM GapDH-SSA was equilibrated with 12.5 μM BrxA, 40 μM BSH and 500 μM NADPH in 20 mM Tris, 1.25 mM EDTA, pH 8.0 at room temperature for 30 min. Next, 12.5 μM YpdA protein was added to the reaction mix at 30 °C for 6 min and NADPH consumption was measured at 340 nm. The biochemical activity assays were each performed in 3–4 replicate experiments.

2.9. GapDH activity assays

GapDH activity assays were performed after allicin exposure using a spectrophotometric assay with glyceraldehyde-3-phosphate (G3P) as substrate and NAD^+ as cofactor to monitor NADH generation as absorbance increase at 340 nm as described [31]. The GapDH reaction mix contained 2.5 μM GapDH, 0.25 mM G3P, 1.25 mM NAD^+, 150 mM sodium arsenate in 20 mM Tris-HCl, 1.25 mM EDTA, pH 8.0. To study GapDH inactivation by allicin *in vitro*, purified GapDH was reduced with 10 mM DTT for 20 min and excess of DTT was removed with Micro Biospin 6 columns. Reduced GapDH was *S*-thioallylated with 0.1–0.75 mM allicin for 10 min at 37 °C, and GapDH activity was measured. For reduction of *S*-thioallylated GapDH, 10 mM DTT or 12.5 μM BrxA were added to GapDH-SSA for 30 min and the regeneration of GapDH activity was monitored in NADH progress curves.

2.10. Western blot analysis

S. aureus strains were grown in LB until an OD_{540} of 2, transferred to Belitsky minimal medium and treated with 150 and 300 μM allicin for 60 min. Cytoplasmic proteins were prepared and subjected to non-reducing BSH-specific Western blot analysis using the polyclonal rabbit *anti*-BSH antiserum as described previously [30].

3. Results

3.1. Allicin provokes a strong thiol-specific oxidative and sulfur stress response in the S. aureus USA300 transcriptome

Growth curves and survival assays were performed to determine the sub-lethal and growth-inhibitory allicin concentration in *S. aureus* COL and USA300. Exposure of *S. aureus* to 100–300 μM allicin during the exponential growth resulted in a lack of growth for 1 h followed by resumption of growth with the same growth rate as in untreated cells (Fig. S1AB). Survival assays in Belitsky minimal medium further revealed no negative effect of 150–300 μM allicin on cell viability of *S. aureus* COL and USA300 (Fig. S1CD). Thus, 300 μM allicin was applied as sub-lethal dose to investigate the changes in the RNA-seq transcriptome in *S. aureus* USA300 in 3 biological replicate experiments before (control) and 30 min after allicin exposure as described previously [38,53]. For significant expression changes, the M-value cut-off (log2-fold change allicin/control) of ≥0.6 and ≤-0.6 (fold-change of ± 1.5, $P \leq 0.05$) was used. Among the differentially transcribed genes, 457 were significantly > 1.5-fold up-regulated and 674 were < -1.5-fold down-regulated under allicin stress (Figs. 1 and 2, Tables S4 and S5). About 58 genes displayed the highest fold-changes (10–268-fold), which belong to the PerR, HypR, QsrR, MhqR, CtsR, HrcA, CidR, CymR, CstR, CsoR, Zur and GraRS regulons. Thus, the transcriptome under allicin stress resembles a thiol-specific oxidative stress signature as previously defined under NaOCl stress [38].

Moreover, the allicin expression profile overlaps strongly with the transcriptome of *S. aureus* under NaOCl [38] and AGXX® stress [39]. The thiol-specific *hypR-merA* operon (HypR regulon) and the *USA300HOU_2567–68* operon are most strongly induced with fold-changes of 195–228 and 220–267, respectively (Figs. 1 and 2, Tables S4 and S5). In addition, the QsrR, CstR, CsoR and Zur regulons showed 20–88-fold transcriptional up-regulations by allicin. The CstR repressor controls the *cstAB-sqr* and *cstR-tauE* operons and senses reactive sulfur species (RSS), such as hydrogen sulfide [54–56]. Thus, the induction of the CstR regulon by allicin supports its main mode of action as RSS [57]. The up-regulation of the CsoR and Zur regulons by allicin might be explained by *S*-thioallylation of metal binding Cys in these metalloregulatory proteins, leading to their inactivation and induction of Cu^+ and Zn^{2+}-uptake systems. In addition, the heat-shock specific chaperones and proteases of the CtsR and HrcA regulons [58,59] were 10–20-fold up-regulated by allicin, including the *ctsR-mcsA-mcsB-clpC* and *hrcA-grpE-dnaKJ* operons. This supports the increased aggregation by *S*-thioallylation of protein thiols, resulting in a protein damage and a heat shock response as demonstrated in *E. coli* [14].

Moreover, allicin has been shown to deplete GSH and protein thiols in *E. coli* and eukaryotic cells [14,18,19]. Thus, it is anticipated that allicin causes depletion of cysteine and BSH in *S. aureus*. In agreement with this notion, the CymR regulon for cysteine biosynthesis and the pathways for BSH biosynthesis and reduction of *S*-bacillithiolated proteins were 2–5-fold induced by allicin, including the *bshA*, *bshB*, *bshC*, *brxA*, *brxB* and *ypdA* genes and operons (Tables S4 and S5). In addition, allicin resulted in increased transcription of members of the GraRS cell wall stress regulon in *S. aureus*. This might be related to allicin's effect on the membrane potential as shown in yeast and the alga *Chara corallina* [21,42]. Finally, allicin led to 11–14-fold induction of genes encoding flavin oxidoreductases, such as *acpD*, *namA* and *nfrA* in *S. aureus*. These could be involved in allicin detoxification or reduction of *S*-thioallylations to regenerate BSH or protein thiols. Taken together, our RNA-seq data support that allicin leads to a strong thiol-specific oxidative and sulfur stress response and protein damage in *S. aureus* USA300, which is probably attributed to *S*-thioallylation of LMW thiols and proteins thiols.

3.2. Northern blot analysis indicates that allicin causes similar thiol-specific stress responses in S. aureus and B. subtilis

Next, we used Northern blot analyses to confirm the induction of thiol-specific regulons by allicin in *S. aureus* USA300. In addition, we were interested whether a similar thiol-specific transcriptional response is caused in the related Gram-positive bacterium *B. subtilis*. Thus, we analyzed the transcription of representative homologous genes of the PerR (*katA*), QsrR/YodB (*azoR1*), CymR (*cysK*) and SarZ/OhrR (*ohr/ohrA*) regulons of *S. aureus* and *B. subtilis* under allicin stress (Fig. 3). The Northern blot results showed strong induction of the genes of the PerR, QsrR/YodB, CymR and SarZ/OhrR regulons in both bacteria, indicating similar thiol-reactive modes of actions of allicin in *S. aureus* and *B. subtilis* (Fig. 3AB). Quantification of the Northern blot signals revealed inductions of 32–63-fold for the YodB/QsrR dependent *azoR1* gene and for the SarZ/OhrR-regulated *ohr/ohrA* genes in both *S. aureus* and *B. subtilis* under allicin treatment (Fig. 3CDE). These results indicate that allicin elicits similar thiol-specific oxidative stress responses in both bacteria.

3.3. Allicin leads to an oxidative shift in E_{BSH} and widespread S-thioallylation of 57 proteins in S. aureus

Next, we investigated the changes in E_{BSH} in *S. aureus* USA300 under allicin stress using our genetically encoded Brx-roGFP2 biosensor [40]. The oxidation degree (OxD) of the Brx-roGFP2 biosensor in *S. aureus* cells was followed after injection of increasing levels of 5–100 μM allicin into the microplate wells (Fig. 4A). Remarkably, low levels of 5–10 μM allicin caused already a strong and fast biosensor oxidation, with an OxD increase from 0.4 to ~0.7 within 20 min. The Brx-roGFP2 biosensor was fully oxidized by 20–100 μM allicin and reached an OxD of 0.8–0.9 after 10 min. However, no recovery of the reduced state of E_{BSH} was measured in allicin-treated cells. To prove the reversibility of Brx-roGFP2 oxidation due to *S*-thioallylation, DTT was added to the oxidized allicin-treated biosensor cells resulting in immediate reduction (Fig. 4BC). In conclusion, these Brx-roGFP2 measurements revealed a strongly increased E_{BSH} upon allicin stress supporting its major impact

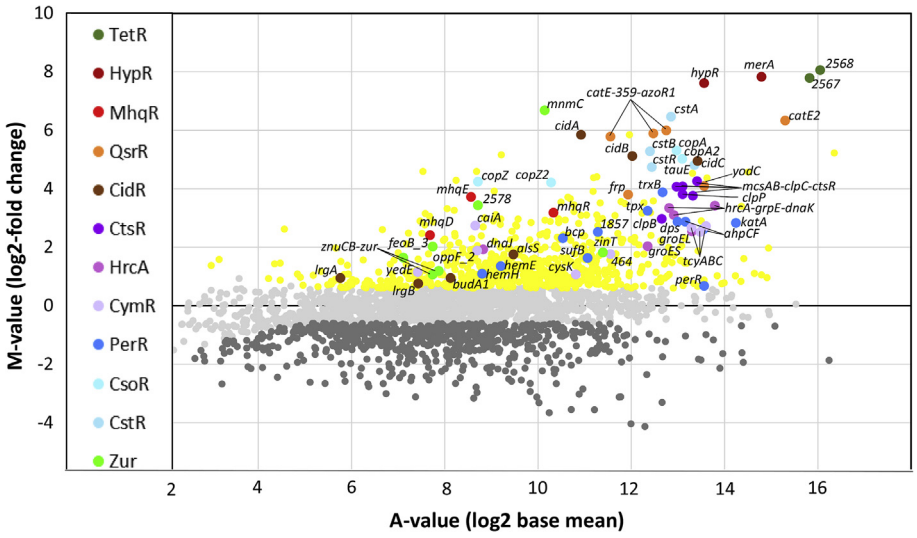

Fig. 1. RNA-seq transcriptomics of *S. aureus* USA300 under allicin stress. For RNA-seq transcriptomics, *S. aureus* USA300 was treated with 300 µM allicin for 30 min. The allicin-induced expression profile is shown as ratio/intensity scatter plot (M/A-plot), which is based on the differential gene expression analysis using DeSeq2. Colored symbols indicate significantly induced (red, orange, yellow, blue, cyan, violet, green, yellow) or repressed (dark grey) transcripts (M-value ≥ 0.6 or ≤ -0.6; P-value ≤ 0.05). Light grey symbols denote transcripts with no fold-changes after allicin stress (P > 0.05). The HypR, TetR, QsrR, PerR, CymR, CtsR, HrcA, Fur, CsoR and CstR regulons are indicative of the thiol-specific oxidative stress response. The RNA-seq data of differential transcription of all genes and regulons under allicin treatment are listed in Tables S4 and S5.

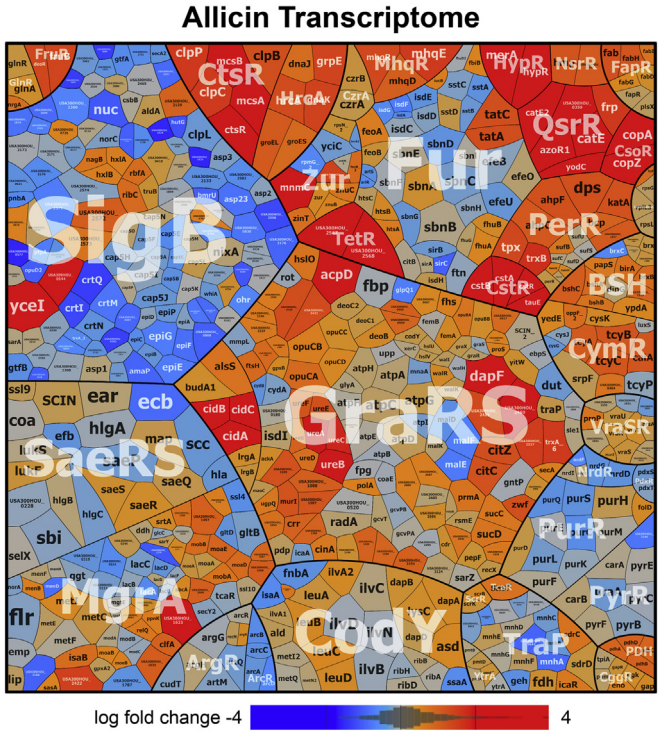

Fig. 2. The transcriptome treemap of *S. aureus* USA300 under allicin stress indicates a strong thiol-specific oxidative stress response. The transcriptome treemap visualizes the differential gene expression of *S. aureus* after exposure to 300 µM allicin as log2 fold changes (M-values). The genes are classified into operons and regulons based on the RegPrecise and Aureowiki databases. Differential gene expression is shown by the red-blue color code where red indicates log2 fold induction and blue repression of transcription under allicin stress. The thiol-specific oxidative stress response is indicated by the induction of the HypR, TetR, PerR, QsrR and CymR regulons. The induction of the CsoR, CstR, Fur, HrcA, CtsR regulons reveals a metal, sulfide and protein damage response in *S. aureus*. The RNA-seq expression data of the genes induced or repressed under allicin exposure and their regulons are listed in Tables S4 and S5.

on the cellular pool of the LMW thiol BSH in *S. aureus*.

Due to the increased E_{BSH} under allicin stress, we next analyzed whether allicin causes S-bacillithiolation of the abundant GapDH protein, as shown previously under HOCl stress [31]. However, BSH-specific Western blot analysis did not reveal increased *S*-bacillithiolation of GapDH or other proteins (Fig. S2). Instead, previous proteomics studies identified widespread protein *S*-thioallylations under allicin stress in *E. coli* and human Jurkat cells [14,18]. Thus, we performed Orbitrap LC-MS/MS analysis of *S. aureus* USA300 cells that were exposed to 300 µM allicin for 30 min to uncover the targets for *S*-thioallylation in *S. aureus*. Proteins with *S*-thioallylations were identified by a mass shift of 72 Da at Cys peptides (Tables S6–S8). In total, we mapped 57 *S*-thioallylated proteins in allicin-treated *S. aureus* cells. These proteins are involved in many cellular pathways, including adaptation to stress, antioxidant functions, energy metabolism, biosynthesis of amino acids, nucleotides and cofactors, transcription, translation and cell wall biosynthesis. The identified *S*-thioallylated Cys peptides were visualized in the Voronoi proteome treemap according to the total spectral counts of protein abundance as quantified with the proteome software Scaffold (Fig. 5). The abundances of 873 proteins could be quantified by spectral counting in the proteome of allicin-treated cells. As expected, the most abundant proteins in the proteome were also *S*-thioallylated, including translation elongation factors (EF-Tu, EF-Ts), ribosomal proteins (RpsB, RpmG_2) and the glutamine synthetase GlnA. However, also lower abundant transcriptional regulators were *S*-thioallylated, such as the MarR/SarA family regulators MgrA, SarA, SarS, SarH1. Among these, MgrA and SarA were modified at their conserved N-terminal Cys12 and Cys9 residues, respectively, that are involved in redox-sensing under oxidative stress [33]. Moreover, the inosine monophosphate (IMP) dehydrogenase GuaB, the manganese-dependent inorganic pyrophosphatase PpaC and the aldehyde dehydrogenase AldA were *S*-thioallylated at their conserved redox-sensing Cys307, Cys158 and Cys279 residues, respectively. GuaB, PpaC and AldA have been previously found *S*-bacillithiolated at their active site Cys residues under NaOCl stress in *B. subtilis* or *S. aureus* [31,60,61]. Among the targets for *S*-thioallylation are also antioxidant enzymes, such as the thiol peroxidase Tpx, the catalase KatA, the bacilliredoxin BrxA and the methionine sulfoxide reductase MsrB. These redox enzymes were *S*-thioallylated at their active site or conserved Cys residues (Tables S6 and S8) and displayed increased oxidations under NaOCl stress in previous OxICAT analyses [31].

To investigate whether allicin modifies conserved Cys residues, we searched all 57 allicin-modified proteins against the database of conserved domains (CDD) (http://www.ncbi.nlm.nih.gov/Structure/cdd/wrpsb.cgi). Interestingly, 37 out of 57 proteins were modified at conserved Cys residues as revealed by CCD, including 14 that harbored *S*-thioallylations at their catalytic active or cofactor binding sites (Tables S6 and S8). Among these are many metabolic enzymes modified at their active site Cys residues, such as the formate dehydrogenase FdhA, the 3-oxoacyl-[acyl-carrier-protein] synthases 2 and 3 (FabH2 and FabH), the

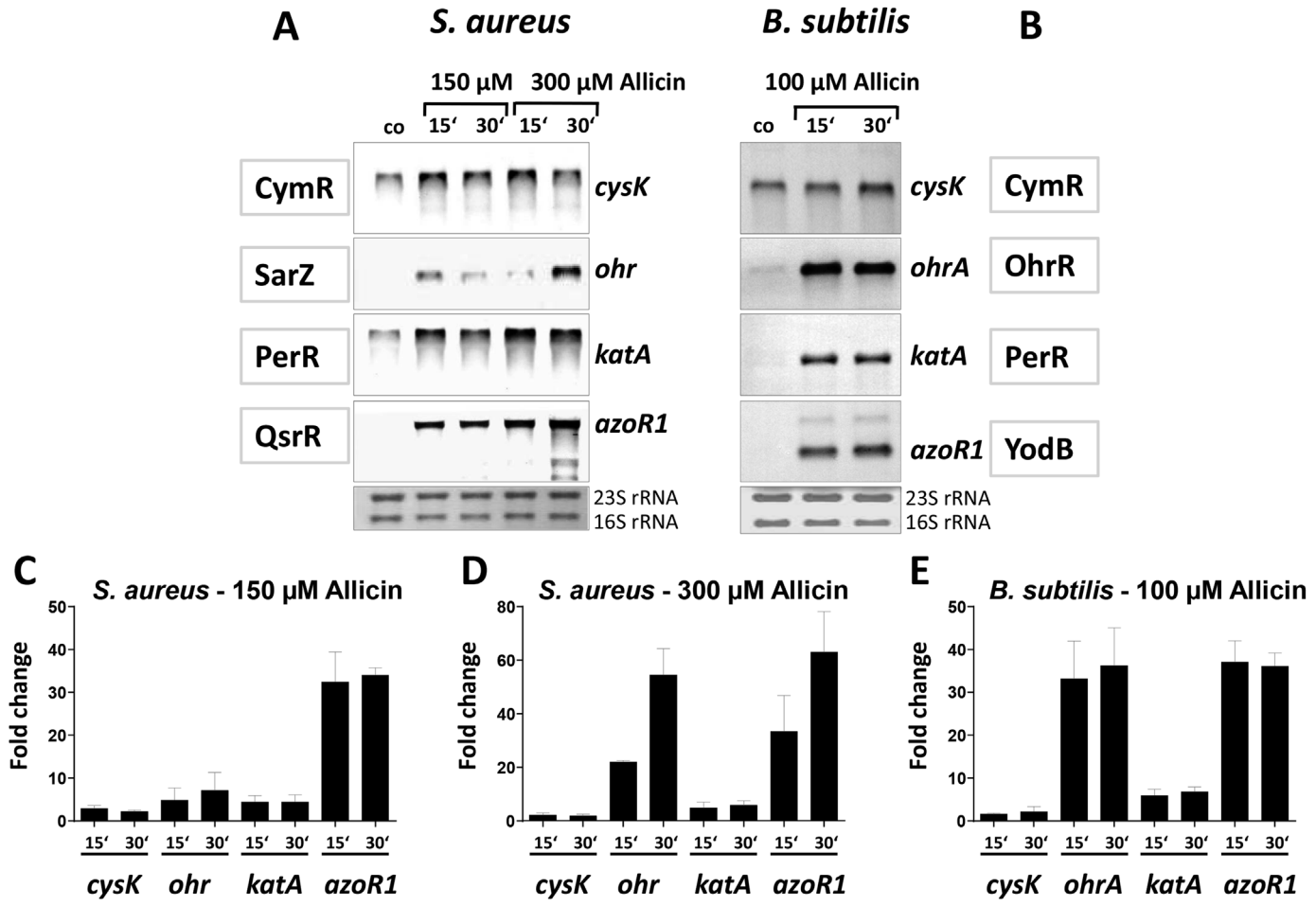

Fig. 3. Northern blot analysis indicates the induction of homologous thiol-stress specific regulons (CymR, OhrR/SarZ, PerR, YodB/QsrR) under allicin treatment in *S. aureus* and *B. subtilis*. Transcription of the genes *cysK, ohr/ohrA, katA* and *azoR1* was analyzed using Northern blots in *S. aureus* USA300 **(A)** and *B. subtilis* **(B)** 30 min after exposure to 150 and 300 µM allicin in *S. aureus* **(A)** or 100 µM allicin in *B. subtilis* **(B)**. The thiol-specific genes *cysK, ohr/ohrA, katA* and *azoR1* are regulated by the CymR, SarZ/OhrR, PerR, QsrR/YodB repressors in *S. aureus* and *B. subtilis,* respectively. The methylene blue stained bands for the 16S and 23S rRNA are indicated at the bottom as RNA loading control. **(C, D, E)** Quantification of the transcriptional induction of *cysK, ohr/ohrA, katA* and *azoR1* after allicin stress in *S. aureus* **(C, D)** and *B. subtilis* **(E)** was performed from the Northern blot images using ImageJ. Allicin-induced fold-changes were calculated from 2-3 biological replicates and error bars represent the standard deviation (SD).

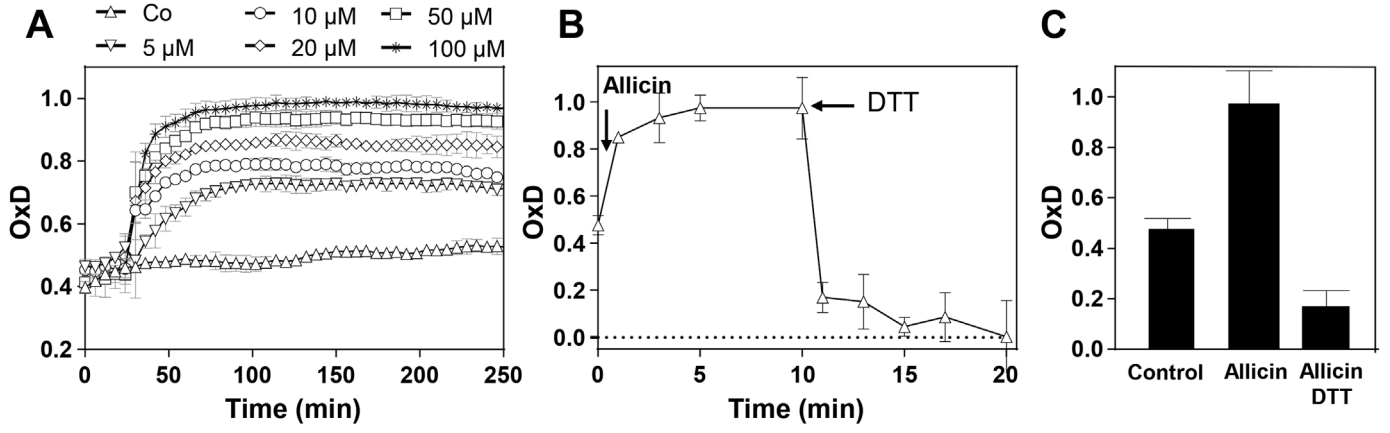

Fig. 4. Brx-roGFP2 biosensor measurements indicate that allicin causes a strong oxidative shift in E_{BSH} of *S. aureus* COL. (A) E_{BSH} of *S. aureus* COL was measured with the Brx-roGFP2 biosensor in *S. aureus* COL after exposure to 5–100 µM allicin using injection assays (see methods). **(B, C)** The Brx-roGFP2 biosensor oxidation and its DTT-reversibility were measured in shake flasks experiments (see methods). Biosensor cells were exposed to 150 µM allicin and harvested at different times (0, 1, 3, 5 and 10 min) after allicin stress to measure the OxD. After 10 min of allicin exposure, 10 mM DTT was added and samples were analyzed to measure Brx-roGFP2 reduction. **C)** The OxD is shown for the untreated control, 10 min after allicin stress and 10 min after allicin treatment followed by 1 min DTT reduction. The OxD was calculated based on 405/488 nm excitation ratios with emission at 510 nm and related to the fully oxidized and reduced controls. The mean values of three biological replicates are shown. Error bars represent the SD.

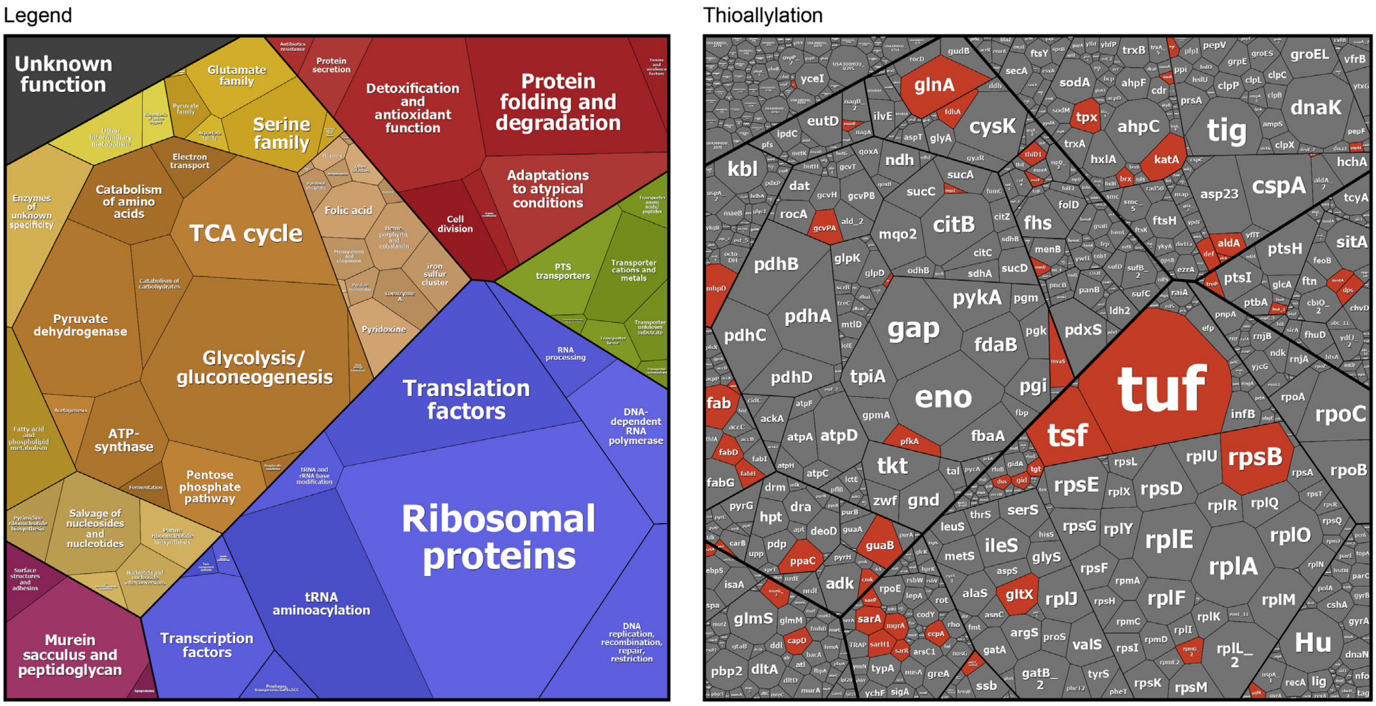

Fig. 5. Allicin leads to *S*-thioallylation of 57 proteins in the *S. aureus* USA300 proteome, which are labelled in red in the proteome abundance treemap. Shotgun LC-MS/MS analysis of total protein extracts was performed that were prepared from allicin-treated *S. aureus* USA300 cells. The cell size indicates the protein abundance in the proteome as quantified by spectral counting of all proteins using the Scaffold proteome software from 3 biological replicates. The identified proteins were classified according to TIGRfam annotation into different functional categories. *S*-thioallylated proteins were labelled in red, which were identified based on the mass shift of 72 Da at Cys residues. The *S*-thioallylated proteins include abundant redox-sensitive antioxidant and metabolic enzymes (AldA, GuaB, PpaC, Tpx, KatA, BrxA, MsrB), translation elongation factors and ribosomal proteins (Tuf, Tsf, RpsB, RpmG_2), but also redox-sensing MarR/SarA-family regulators (MgrA, SarA, SarH1, SarR).

PTS trehalose and fructose/mannitol transporter IIBC components (TreP and FruA), the hydroxymethylglutaryl-CoA synthase (MvaS) and the sortase (SrtA). Taken together, our shotgun proteomics data revealed that allicin causes widespread *S*-thioallylation in *S. aureus*, which includes many redox-sensitive antioxidant enzymes, transcriptional regulators and metabolic enzymes that could be involved in detoxification and regulate cellular adaptation to recover from allicin stress.

3.4. Bacillithiol, the HypR-controlled disulfide reductase MerA and the BrxA/BSH/YpdA redox pathway provide protection against allicin stress in S. aureus

Proteomics and redox biosensor measurements revealed that allicin causes depletion of BSH and protein thiols by *S*-thioallylation in *S. aureus*. To investigate the role of BSH in allicin protection, we analyzed the growth and survival of the *bshA* mutant in comparison to the wild type under allicin stress. The *bshA* mutant showed a strong growth and survival defect after exposure to 100–300 μM allicin stress (Fig. 6). While the wild type quickly recovered in growth after 30–60 min of allicin stress, the *bshA* mutant showed a delayed resumption of growth with 100–200 μM allicin (Fig. 6AB) and a decreased optical density with 300 μM allicin (Fig. 6C). The survival of the *bshA* mutant was also significantly impaired after exposure to 200–300 μM allicin compared to the wild type (Fig. 6DE). These results suggest that BSH plays an important role in the detoxification of allicin in *S. aureus*.

The *hypR-merA* operon was most strongly 195–228-fold induced under allicin stress (Table S4), which encodes for the disulfide stress-specific redox regulator HypR and the NADPH-dependent flavin disulfide reductase MerA in *S. aureus* [38]. To investigate the role of MerA in allicin detoxification, we performed growth and survival assays of the *S. aureus* COL wild type, the *merA* mutant and the *merA* complemented strain (Fig. 7, Fig. S3). The *merA* mutant showed a significant growth delay after treatment with 100–200 μM allicin (Fig. 7AB) and was unable to recover in growth after 300 μM allicin stress (Fig. 7C). While the *merA* mutant was also more sensitive in survival assays with 200 μM allicin (Fig. 7D), only a slightly reduced survival was noted with 300 μM allicin in the *merA* mutant (Fig. 7E). The growth and survival defect of the *merA* mutant under allicin stress could be restored back to wild type levels with plasmid-encoded *merA* (Fig. S3). These results indicate that MerA could function as NADPH-dependent disulfide reductase in allicin detoxification.

Furthermore, the genes of the BrxAB/BSH/YpdA pathway showed elevated transcription in the allicin transcriptome (Table S4). We have recently shown that YpdA functions as BSSB reductase in *S. aureus in vitro* and acts together with the BrxAB pathway in de-bacillithiolation of proteins under HOCl stress [41]. Thus, it is possible that *S*-thioallylated proteins are also recycled by the BrxAB/BSH/YpdA pathway. To investigate the role of the BrxAB/BSH/YpdA pathway in the allicin stress response, we analyzed the growth of the *brxAB* and *ypdA* mutants and their respective *ypdA*, *brxA* and *brxB* complemented strains under allicin exposure (Fig. 8). The growth of both, *ypdA* and *brxAB* mutants was significantly impaired after treatment with 200 μM allicin (Fig. 8AB). This growth deficiency of the mutants could be rescued in the *ypdA*, *brxA* and *brxB* complemented strains (Fig. 8C–E). These results indicate that the BrxAB/BSH/YpdA pathway could function in regeneration of *S*-thioallylated proteins under allicin stress. In this Brx redox pathway, YpdA should be involved in BSSA reduction, formed upon BrxAB regeneration with BSH.

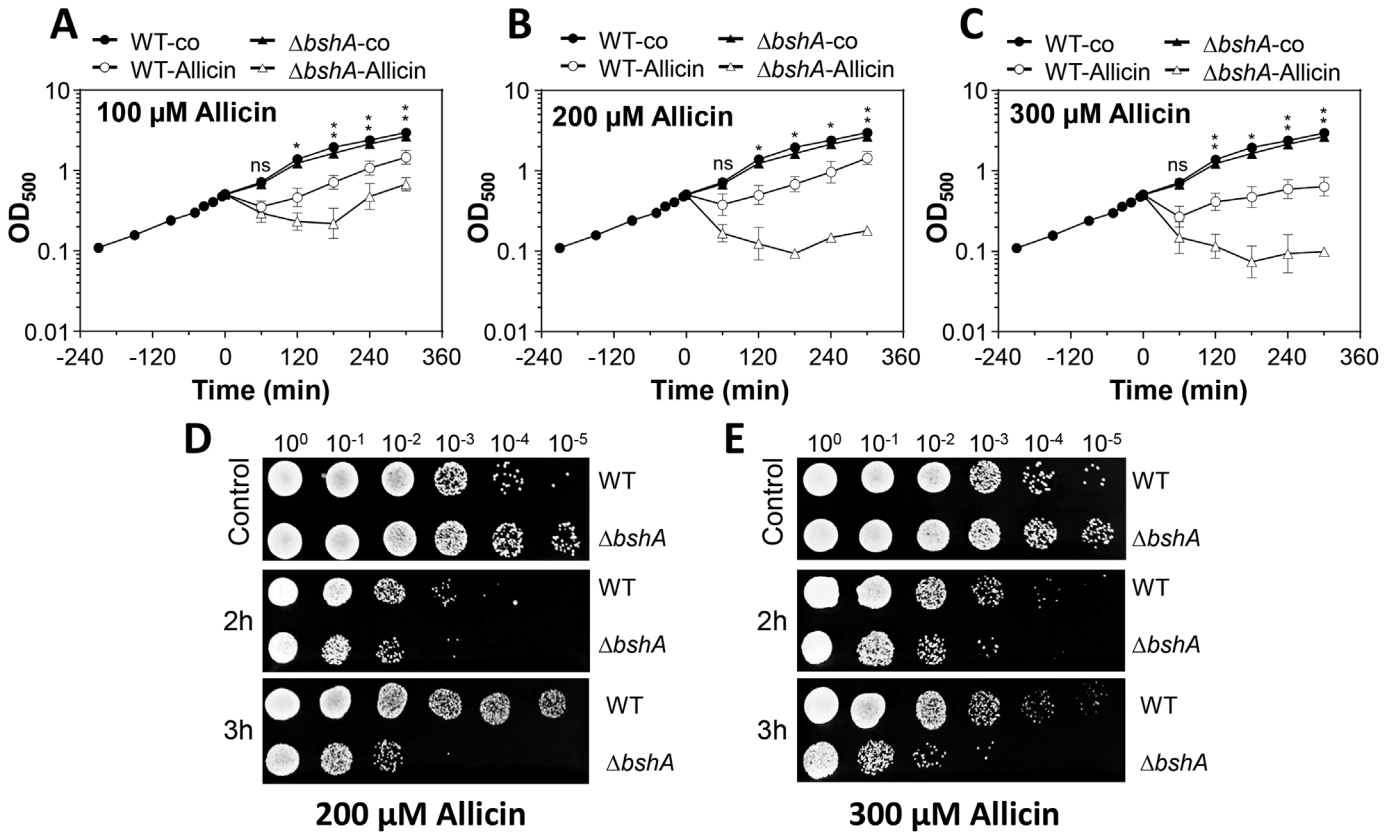

Fig. 6. BSH is involved in detoxification of allicin in *S. aureus* COL. Growth phenotype analyses **(A–C)** and survival assays **(D, E)** of the *S. aureus* COL wild type (WT) and the *bshA* mutant before and after treatment with 100–300 µM allicin stress at an OD_{500} of 0.5. **(D, E)** Survival assays were performed by spotting 10 µl of serial dilutions after 2 and 3 h of exposure to 200–300 µM allicin onto LB agar plates. The results are from 3 biological replicate experiments. Error bars represent the SD and the statistics was calculated using a Student's unpaired two-tailed *t*-test by the graph prism software. Symbols are defined as follows: $^{ns}p > 0.05$, $^{*}p \leq 0.05$ and $^{**}p \leq 0.01$.

3.5. Biochemical assays indicate that MerA functions in allicin detoxification, YpdA is involved in BSSA reduction and the BrxA/BSH/YpdA pathway catalyzes reversal of protein S-thioallylations

Next, we investigated the functions of MerA and YpdA in allicin and BSSA reduction using NADPH-coupled progress curves *in vitro*. Purified MerA and YpdA both consumed little NADPH *in vitro* without substrates (Fig. 9AB). Increasing levels of 125–250 µM allicin significantly stimulated consumption of NADPH by MerA (Fig. 9A). However, NADPH-consumption by MerA was only slightly increased with BSSA as substrate, which is formed by BSH and allicin, indicating that MerA is specific for allicin reduction (Fig. 9C). The allicin reductase activity of MerA was dependent on the Cys43xxxxCys48 active site, since replacements of Cys43 by serine abolished NADPH consumption with allicin (Fig. 9A). Thus, MerA functions as allicin defense mechanism catalyzing its reduction to restore normal growth. Interestingly, the previously characterized BSSB reductase YpdA [41,62] showed strongly increased NADPH consumption with BSSA as substrate, indicating that YpdA can recycle the BSH moiety from BSSA (Fig. 9B). For control purposes, we repeated the reaction of YpdA with its natural substrate BSSB as revealed in the previous study [41] (Fig. 9B). YpdA showed a similar level of NADPH consumption with both substrates BSSB and BSSA, further verifying that YpdA can function as BSSA reductase. The BSSA reductase activity of YpdA was further dependent on the conserved Cys14 residue, located in the GGGxCG Rossman-fold motif involved in NADPH binding (Fig. 9B). However, NADPH consumption by YpdA was not increased with allicin as substrate, supporting that YpdA cannot detoxify allicin (Fig. 9D). Taken together, biochemical NADPH coupled assays revealed that MerA is involved in allicin reduction, while YpdA specifically reduces BSSA in allicin-treated cells.

We were further interested if proteins are inactivated by *S*-thioallylation and if the BrxA/BSH/YpdA pathway can catalyze its reversal. Since GapDH activity was previously inhibited by *S*-bacillithiolation [31], we used GapDH as model to study the effect of allicin on its inactivation and its reversibility. Incubation of GapDH with 0.5–0.75 mM allicin resulted in a 75–99% activity decrease, which could be regenerated to 56% with 10 mM DTT (Fig. 10A–D). Reduction of *S*-thioallylated GapDH with BrxA restored only 27% of GapDH activity. This low recovery of GapDH activity by BrxA is probably due to BrxA inactivation by allicin. Thus, we used NADPH coupled assays with the BrxA/BSH/YpdA electron pathway for reduction of *S*-thioallylated GapDH and measured NADPH consumption. Progress curves revealed a significantly decreased absorbance due to NADPH oxidation in the presence of *S*-thioallylated GapDH with the complete BrxA/BSH/YpdA electron pathway (Fig. 10E). These results lead to the conclusion that BrxA facilitates recycling of *S*-thioallylated proteins, resulting in BrxA-SSA formation. BrxA-SSA is regenerated by BSH, leading to BSSA formation. BSSA is the substrate for YpdA, which rescues BSH on expense of NADPH (Fig. 11). Together our phenotype results and biochemical data revealed that BSH and MerA are involved in allicin detoxification, while BSSA is the substrate for YpdA. The Brx/BSH/YpdA pathway functions in regeneration of *S*-thioallylated proteins in *S. aureus*.

4. Discussion

Allicin is the major organosulfur compound produced in garlic tissue upon wounding [10]. Allicin and garlic-derived diallyl polysulfanes have been shown to exert their antimicrobial and toxic effects

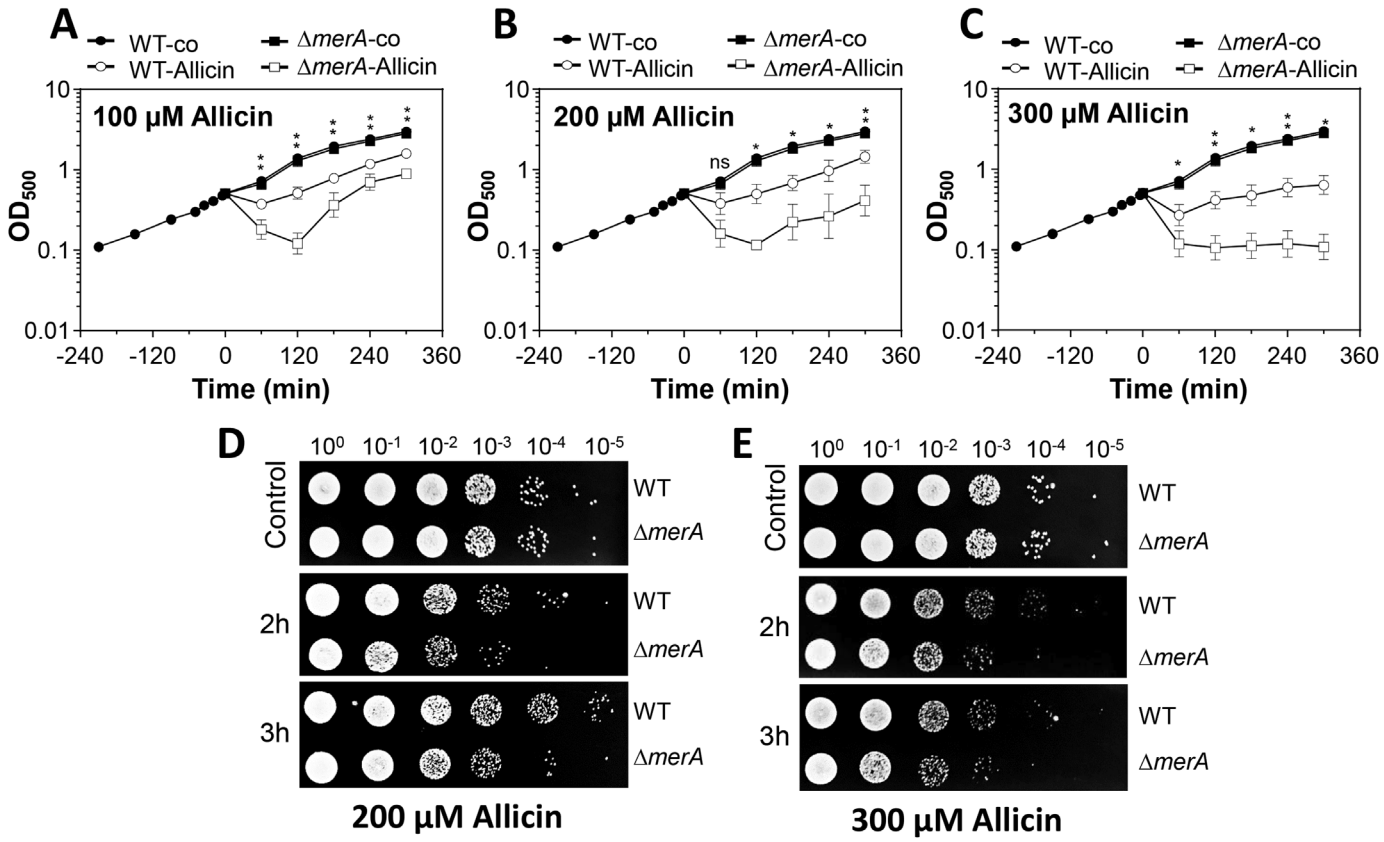

Fig. 7. The *S. aureus merA* mutant shows increased sensitivity under allicin stress. Growth curves **(A–C)** and survival assays **(D, E)** of *S. aureus* COL WT and the *merA* mutant after exposure to allicin stress. The cells were grown in RPMI medium until an OD_{500} of 0.5 and treated with 100–300 µM allicin. **(D, E)** Survival was analyzed for *S. aureus* COL WT and the *merA* mutant by plating serial dilutions after 2 and 3 h of exposure to 200–300 µM allicin on agar plates. One representative experiment of 3–4 biological replicates is shown for the survival assay. Error bars for the growth curves in A-C indicate the SD and the statistics was calculated using a Student's unpaired two-tailed *t*-test by the graph prism software. Symbols are: $^{ns}p > 0.05$, $^{*}p \leq 0.05$ and $^{**}p \leq 0.01$.

through *S*-thioallylation of protein and LMW thiols in different organisms, including *E. coli*, *B. subtilis*, yeast and human Jurkat cells [10,14,16,18,19]. In this work, we applied RNA-seq transcriptomics, proteomics, E_{BSH} measurements, mutant phenotype analyses and biochemical assays to unravel allicin's mode of action in *S. aureus* and to elucidate defense mechanisms for allicin detoxification and reversal of *S*-thioallylations from BSH and proteins.

In support of its thiol-reactive mode of action, allicin provoked a strong oxidative and disulfide stress response in the RNA-seq transcriptome, as shown by the induction of the HypR, PerR, QsrR, MhqR, CsoR and CstR regulons. The redox-sensing Rrf2-family repressor HypR was shown to control the flavin disulfide reductase MerA, which responds to disulfide stress, provoked by HOCl, AGXX®, diamide and allicin [38,39]. Thus far, the function and substrate of MerA was unknown. NADPH coupled assays revealed that MerA functions in direct allicin detoxification, since NADPH consumption was stimulated. In addition, the *merA* mutant displayed strong sensitivity under allicin stress in growth and survival assays. Thus, *merA* was among the top hits in the allicin transcriptome (228-fold induced), and plays a major role in detoxification of allicin *in vitro* and *in vivo*.

Of further importance is the induction of the CstR regulon in the RNA-seq transcriptome, which specifically responds to RSS, such as hydrogen sulfide (H_2S) in *S. aureus* [54–56]. The CstR repressor controls the *cstAB* operon that encodes for thiosulfate sulfurtransferase and persulfide dioxygenase-sulfurtransferase involved in detoxification of RSS [63,64]. Allicin decomposition results in persulfides and polysulfanes explaining the strong induction of the sulfur specific CstR regulon. Overall, the thiol-specific transcriptome signature of the HypR, PerR and QsrR regulons by allicin overlaps strongly with the expression profile by other strong oxidants, which cause disulfide stress, such as the microbicidal oxidant HOCl [38] and the AGXX® antimicrobial surface coating, which produces hydroxyl radicals [39]. Transcription of the cell wall stress responsive GraRS regulon was further enhanced under allicin, HOCl and AGXX® treatment in *S. aureus* [38,39]. Thus, allicin causes strong disulfide stress, similar as the thiol-reactive compounds HOCl and diamide.

The common modes of actions of allicin, diamide and HOCl have been recognized in *E. coli* [14]. Allicin acts mainly via *S*-thioallylation of LMW thiols and protein thiols, which impairs the intracellular thiol-redox balance and protein homeostasis. Thus, the CtsR and HrcA-regulons are highly induced by allicin, which regulate protein homeostasis through the GroESL and DnaK chaperones and ClpB/C/P proteases. Chaperones and Clp proteases are involved in protein folding and degradation of oxidatively unfolded and aggregated proteins [58,59,65,66]. Protein aggregation and widespread *S*-thioallylation of proteins was demonstrated in *E. coli* cells under allicin stress, leading to induction of the heat shock RpoH regulon, which is controlled by stabilization of the RpoH sigma factor [14]. Thus, allicin leads to strong induction of the heat and oxidative shock response due to protein *S*-thioallylation in both *E. coli* and *S. aureus*.

Previous studies demonstrated the strong depletion of the LMW thiol GSH in *E. coli*, yeast and human cells by *S*-thioallylation resulting in GSSA formation [14,18,42]. Accordingly, an oxidative shift in the GSH redox potential (E_{GSH}) from −251 to −181 mV was measured using the genetically encoded roGFP2 biosensor in yeast cells [42]. In *S. aureus,* a strong oxidative shift in E_{BSH} was monitored with the Brx-roGFP2 biosensor after treatment with 5–20 µM allicin, while higher doses of 50–100 µM allicin led to complete biosensor oxidation. These

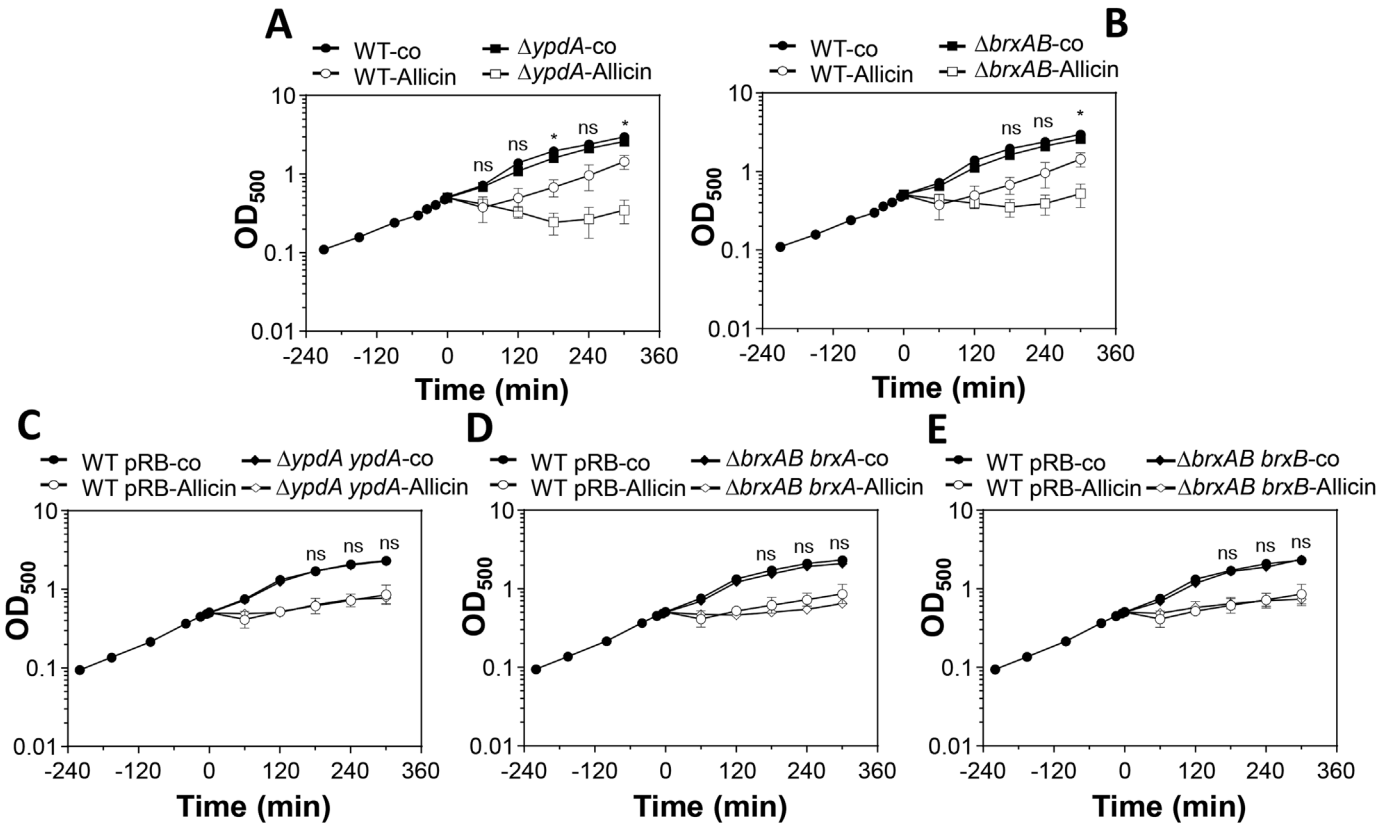

Fig. 8. The *S. aureus ypdA* and *brxAB* mutants display increased susceptibilities to allicin stress, which can be rescued in the *ypdA*, *brxA* and *brxB* complemented strains. Growth curves were monitored in RPMI medium for the *S. aureus* COL WT, the *ypdA* and *brxAB* mutants **(A, B)** as well as in the *ypdA*, *brxA* and *brxB* complemented strains **(C, D, E)** after treatment with 200 μM allicin at an OD_{500} of 0.5. The results are from 2 biological experiments with each 3 technical replicates. Error bars indicate the SD and the statistics was calculated using a Student's unpaired two-tailed *t*-test by the graph prism software. Symbols are: $^{ns}p > 0.05$, $*p \leq 0.05$ and $**p \leq 0.01$.

results confirm the depletion of reduced BSH and the oxidation of BSH to *S*-thioallyl-BSH conjugates, which changes the BSH redox state. Surprisingly, *S. aureus* cells were unable to regenerate reduced E_{BSH} in the biosensor injection assays indicating the strong thiol-reactivity of micromolar allicin. However, reduced E_{BSH} could be regenerated with DTT pointing to the formation of BSSA, which is responsible for the oxidative shift in E_{BSH} upon allicin exposure.

The very fast uptake of the volatile compound allicin and its strong GSH depletion has been shown in *E. coli*, yeast and human cells [14,18,42]. Allicin can easily penetrate the phospholipid membrane, causing pore formation in biological membranes and artificial lipid bilayers [20,21]. However, despite the strong BSH depletion, *S. aureus* wild type cells were able to recover quickly from allicin-induced growth arrest. After 1 h of exposure of *S. aureus* to 100–200 μM allicin, growth was resumed with the same growth rate as untreated control cells. The same growth behavior was found in *E. coli* cells upon treatment with 128 μg/ml allicin, indicating that bacteria are able to detoxify allicin fast and efficiently [14]. In addition, bacteria must encode efficient reducing systems to remove *S*-thioallylated adducts from LMW thiols and protein thiols.

Reduction of GSSA by the glutathione disulfide (GSSG) reductase was recently shown in yeast cells, although GSSA is *in vitro* a poorer substrate (K_m = 0.5 mM) than GSSG (K_m = 0.07) [67]. In *E. coli*, GSSA might be also a substrate for the GSSG reductase Gor. Under oxidative stress, GSH is usually oxidized to GSSG resulting in a decreased GSH/GSSG redox ratio and an increased E_{GSH}. Gor restores the GSH/GSSG redox balance by reduction of GSSG to GSH on expense of NADPH [68,69]. However, GSH depletion by allicin was caused by *S*-thioallylation, and the amount of GSSG was strongly decreased in *E. coli*, leading to a higher GSH/GSSG redox ratio [14]. This indicates that GSH plays an important role in allicin detoxification leading to GSSA. In support of this notion, GSH-deficient mutants in yeast lacking the *GSH1* gene for the γ-glutamyl cysteine synthase were impaired in growth under allicin stress [67,70]. Similarly, BSH was shown to function in allicin detoxification in our phenotype analyses since the BSH-deficient mutant was impaired in growth and survival under allicin stress. Thus, we conclude that bacterial LMW thiols confer resistance to allicin by direct conjugation forming *S*-allylmercapto modified LMW thiols.

Bacteria may use similar pathways for recycling of *S*-thioallylated LMW thiols, involving NADPH-dependent flavin disulfide reductases (FDR), such as Gor and TrxB. The NADPH-dependent FDR YpdA was recently shown to function as BSSB reductase and plays an important role in the defense of *S. aureus* against HOCl and H_2O_2 stress as well as in infection assays with neutrophils and macrophages [41,62]. In this study, the *ypdA* mutant was also strongly impaired in growth and survival under allicin stress, pointing to the role of YpdA in BSSA reduction. Biochemical NADPH coupled assays revealed that YpdA consumed more NADPH when exposed to BSSA compared to NADPH alone, providing further support for its role in reduction of BSSA *in vitro*. Thus, we identified another important function of YpdA in regeneration of reduced BSH upon allicin stress.

Apart from BSSA formation, allicin caused widespread *S*-thioallylation of 57 proteins in *S. aureus* as revealed by shotgun LC-MS/MS analysis. These *S*-thioallylated proteins include several highly abundant proteins, such as translation elongation factors (EF-Tu, EF-Ts), ribosomal proteins (RpsB, RpmG2) and metabolic enzymes (GlnA). Similarly, widespread *S*-thioallylations of 332 proteins was detected in human Jurkat cells, including highly abundant cytoskeletal proteins (actin, tubulin, filamin, cofilin, plastin-2), chaperones (HSP90AB1), translation elongation factors (EEF2) and glycolytic enzymes (GAPDH,

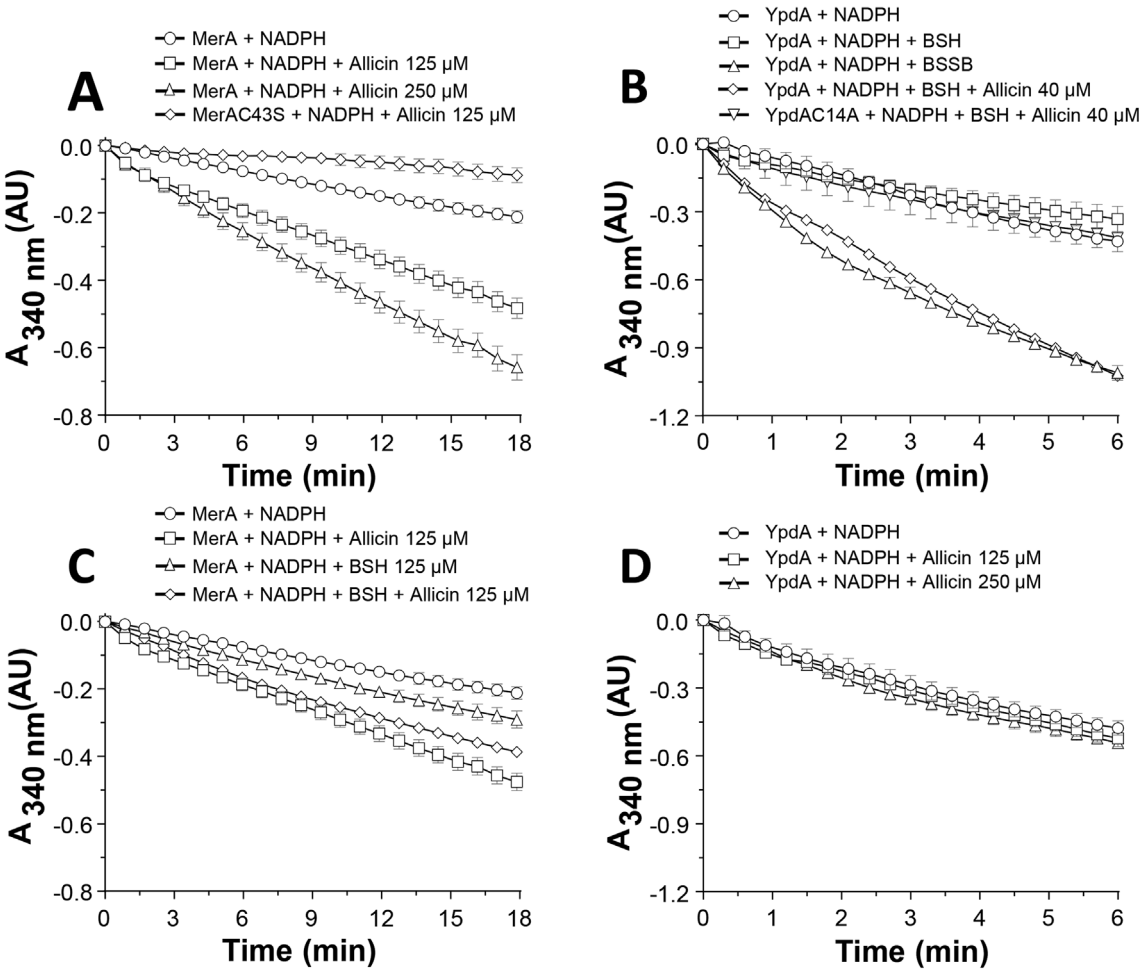

Fig. 9. NADPH coupled assays for allicin detoxification by MerA and reduction of *S*-allylmercaptobacillithiol (BSSA) by YpdA. (A) Purified MerA is able to reduce allicin using NADPH as electron source as measured in progress curves by the absorbance decrease at 340 nm. Control reactions showed little NADPH consumption with MerA alone without allicin or in the MerAC43S active site mutant. **(B)** Purified YpdA functions in BSSA reduction as shown by increased NAPDH consumption in the progress curves, but the YpdAC14A active site mutant is unable to reduce BSSA. For control purposes, the previously determined NADPH-dependent reaction of YpdA with its substrate BSSB [41] was measured again in this study showing the same absorbance decrease as with BSSA. **(C)** NADPH consumption was only slightly stimulated by MerA with BSSA as substrate indicating that MerA is primarily involved in allicin detoxification. **(D)** Allicin is no substrate for YpdA, since NADPH consumption was not increased. Thus, MerA functions in detoxification of allicin and YpdA catalyzes reduction of BSSA using their conserved active site Cys residues.

ALDOA, PKM) as most strongly *S*-thioallylated proteins [18]. In *E. coli*, *S*-thioallylated proteins were identified as abundant metabolic enzymes [14]. In many cases, allicin did not modify catalytic or redox-sensitive Cys residues, but instead non-specifically accessible cysteines in the *E. coli* proteome [14]. However, in the allicin proteome of *S. aureus*, we detected many low abundant redox-sensitive transcription factors of the MarR/SarA family, such as SarA, MgrA, SarR and SarH1 that were modified at their redox-sensing Cys residues [33]. In total, 37 out of 57 proteins were *S*-thioallylated at conserved Cys residues, including 14 at their catalytic, redox-sensitive active site Cys. Moreover, we found an overlap of 16 *S*-thioallylated Cys peptides with those detected with the OxICAT method in HOCl stressed cells [31]. For example, GuaB and AldA displayed the highest oxidation increase of ~29% in the OxICAT analysis and were *S*-bacillithiolated at their redox-sensitive active site Cys307 and Cys279 in HOCl-stressed cells, respectively [31,60,61]. GuaB and AldA were also modified by allicin at their redox-sensitive active sites.

Although GapDH was previously identified as main target for *S*-bacillithiolation under HOCl stress [31], we failed to detect significantly *S*-thioallylated GapDH in allicin-treated cells by mass spectrometry, possibly due to the large size of the allicin modified Cys151 peptide, which was only found with low Xcorr scores (data not shown). However, we could show that purified GapDH was reversibly inactivated by *S*-thioallylation *in vitro*. GapDH activity was previously inhibited by *S*-bacillithiolation, which functions in redox-regulation and thiol-protection against irreversible overoxidation to Cys sulfonic acid [28,31]. Thus, *S*-thioallylation by sub-lethal allicin doses might also function in redox regulation and thiol-protection in *S. aureus* to avoid overoxidation of essential Cys residues.

The widespread *S*-thioallylation of 57 proteins raises the question about the pathways for regeneration. In principle, *S*-thioallylations are mixed protein disulfides, which could be reversed by thioredoxins and glutaredoxins in eukaryotes [18]. In *S. aureus*, the RSS Na_2S caused widespread *S*-sulfhydrations (R–SSH) in the proteome. In addition, *S*-sulfhydration of GapDH could be regenerated by the novel thioredoxins (TrxP and TrxQ) [56]. Among the *S*-thioallylated proteins, we identified the bacilliredoxin BrxA, which could be involved in reduction of *S*-thioallylated proteins. The BrxA/BSH/YpdA pathway was recently characterized to catalyze de-bacillithiolation of GapDH [31,41]. Thus, we used GapDH as substrate for *S*-thioallylation by allicin *in vitro* to study its reversal by the BrxA/BSH/YpdA electron pathway. Interestingly, our results revealed that BrxA could catalyze reduction of *S*-thioallylated GapDH to restore GapDH activity. Moreover, NADPH coupled electron transfer assays with the BrxA/BSH/YpdA pathways

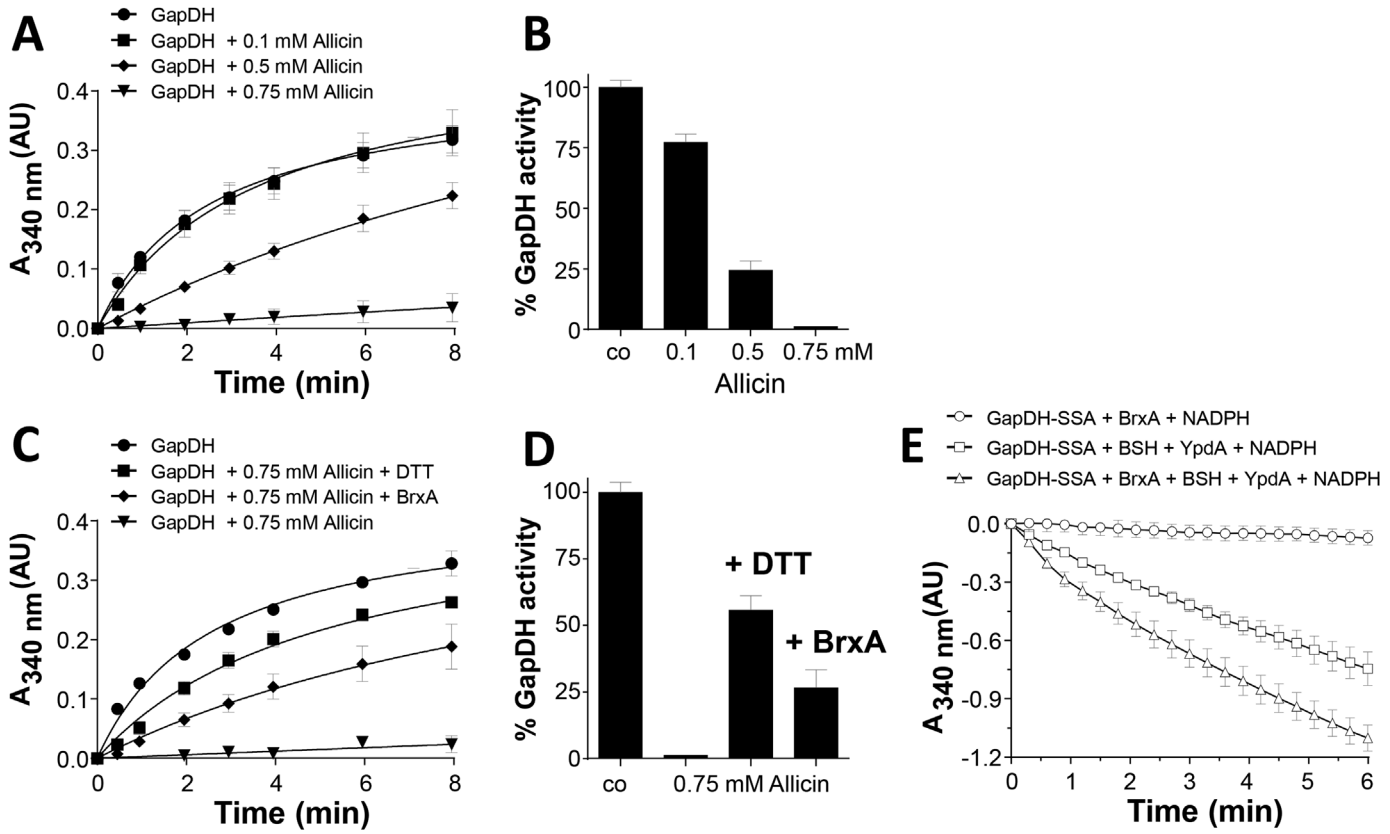

Fig. 10. Inactivation of GapDH in *S. aureus* by *S*-thioallylation and its reversal by the BrxA/BSH/YpdA pathway *in vitro*. **(A)** Purified GapDH is inactivated by increasing allicin concentrations (0.5–0.75 mM) as measured in GapDH activity assays with G3P as substrate and NAD^+ as cofactor to monitor NADH generation as absorbance change at 340 nm. **(B)** The percentage of GapDH activity upon allicin treatment was measured from the slope of the GapDH reactions in A). **(C)** *S*-thioallylated GapDH can be reactivated with DTT and partially with BrxA. The NADH production is measured in the GapDH activity assays as absorbance change at 340 nm. **(D)** Reduction of *S*-thioallylated GapDH with DTT and BrxA leads to 56% and 27% recovery of GapDH activity as measured from the slope of the GapDH reactions in C). **(E)** Reduction of *S*-thioallylated GapDH was also analyzed in the coupled BrxA/BSH/YpdA electron pathway following NADPH consumption. Fast NADPH consumption was measured with YpdA in the BrxA/BSH coupled assay for de-thioallylations of GapDH-SSA. The coupled assays were conducted with 2.5 μM GapDH-SSA, 12.5 μM BrxA, 40 μM BSH, 500 μM NADPH in 20 mM Tris, 1.25 mM EDTA, pH 8.0. After 30-min incubation at room temperature, 12.5 μM YpdA was added to the reaction mix and NADPH consumption was monitored at 340 nm as a function of time. Mean values and SEM of 3–4 independent experiments are shown.

revealed increased NADPH consumption upon reduction of *S*-thioallylated GapDH. These results confirm that BrxA removes *S*-thioallylations, leading to *S*-thioallylated BrxA (BrxA-SSA), which is reduced by BSH resulting in BSSA formation. BSSA is a substrate for YpdA, which uses electrons from NADPH for BSH regeneration (Fig. 11). The importance of the Brx/BSH/YpdA pathway for the defense of *S. aureus* against allicin was also confirmed *in vivo*. In phenotype assays, both *brxAB* and *ypdA* mutants were strongly impaired in growth and survival under allicin stress. The growth and survival phenotypes of the *brxAB* mutant could be restored with plasmid-encoded BrxA and BrxB, indicating that both bacilliredoxins are involved in de-thioallylation. Thus, our biochemical and mutant phenotype analyses revealed the main role of the BrxAB/BSH/YpdA pathway to regenerate *S*-thioallylated proteins in *S. aureus*.

Taken together, our results revealed that allicin causes a strong thiol-specific oxidative stress and sulfur stress response and protein damage in the transcriptome of *S. aureus* USA300 as revealed by the up-regulation of the HypR, PerR, QsrR, CstR, CtsR and HrcA regulons. The antimicrobial and toxic effect of allicin is mainly attributed to its fast reaction with LMW and protein thiols, leading to a strong oxidative shift in E_{BSH} and widespread *S*-thioallylations in the *S. aureus* proteome. We further revealed that BSH and MerA are involved in direct allicin detoxification, while the recently characterized BSSB reductase YpdA functions in BSSA reduction. In addition, the BrxA/BSH/YpdA pathway catalyzes the removal of *S*-thioallylations from proteins. Thus, BSH, MerA and the BrxA/BSH/YpdA pathway function together in allicin removal to restore the thiol-redox homeostasis in allicin-treated *S. aureus* cells. Due to the multiple cellular targets and its volatile nature, allicin is an attractive antimicrobial compound and potential lead substance to develop therapies to combat life-threatening MRSA infections.

Author disclosure statement

No competing financial interests exist.

Acknowledgements

We are thankful to Ambrose Cheung (Dartmouth College) for providing the *S. aureus* USA300 *bshA* mutant and to Chris J Hamilton for providing BSH and BSSB. This work was supported by an European Research Council (ERC) Consolidator grant (GA 615585) MYCOTHIOLOME and grants from the Deutsche Forschungsgemeinschaft, Germany (AN746/4–1 and AN746/4–2) within the SPP1710 on “Thiol-based Redox switches”, by the SFB973 (project C08) and TR84 (project B06) to H.A. Further support for allicin synthesis was provided by internal funding from the RWTH Aachen University to M.C.H.G. and A.J.S.

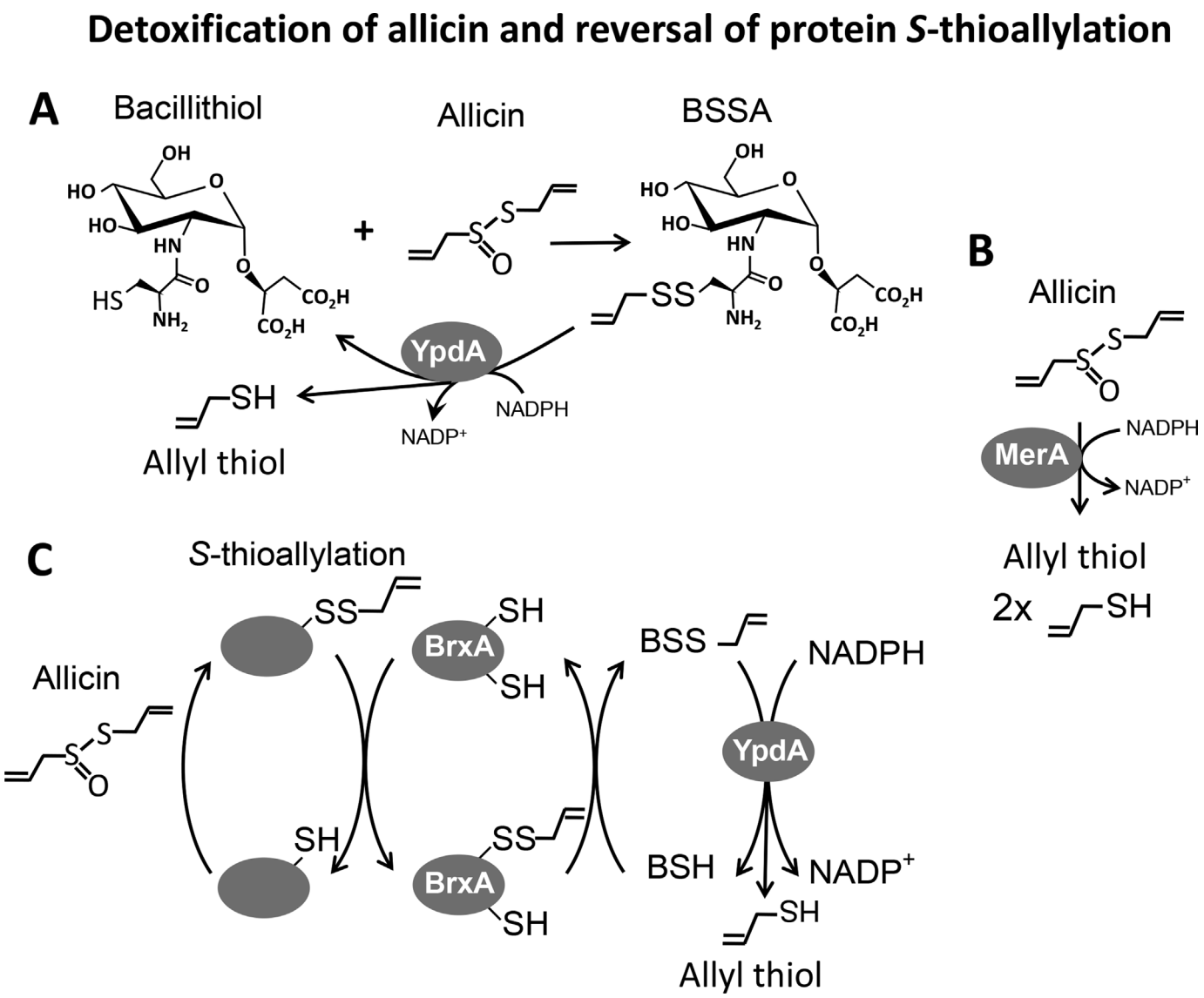

Fig. 11. Detoxification of allicin by BSH (A) and MerA (B) and reversal of *S*-thioallylation of proteins by the BrxA/BSH/YpdA pathway (C) in *S. aureus*. The *bshA*, *merA*, *ypdA* and *brxAB* mutants showed strong growth defects under allicin treatment in *S. aureus in vivo* indicating their function in allicin detoxification and reversal of protein *S*-thioallylation. Allicin caused an oxidative shift in E_{BSH}, which is caused by formation of mixed disulfides between BSH and allicin, leading to *S*-allylmercaptobacillithiol (BSSA) **(A)**. Biochemical coupled assays revealed that MerA could detoxify allicin due to consumption of NADPH **(B)**, but YpdA could not detoxify allicin. In addition, allicin caused *S*-thioallylations of protein thiols, which could be reduced with electrons from the BrxA/BSH/YpdA pathway on expense of NADPH **(C)**. In these BrxA/BSH/YpdA coupled assays, BrxA reduces *S*-thioallylated proteins, leading to *S*-thioallylation of BrxA. *S*-thioallylated BrxA is regenerated by BSH to form BSSA as substrate of YpdA. YpdA was previously shown to function as BSSB reductase [41,62], but could also reduce BSSA to regenerate BSH using NADPH as electron donor.

List of abbreviations

BSH	bacillithiol
BSSB	bacillithiol disulphide
BSSA	*S*-allylmercaptobacillithiol
Brx	bacilliredoxin
Brx-roGFP2	Brx fused to roGFP2
CFU	colony forming unit
DTT	dithiothreitol
E_{BSH}	bacillithiol redox potential
E_{GSH}	glutathione redox potential
FDR	flavin disulfide reductase
GapDH	glyceraldehyde-3-phosphate dehydrogenase
GSH	glutathione
GSSG	glutathione disulfide
GSSA	*S*-allylmercaptoglutathione
H_2O_2	hydrogen peroxide
HOCl	hypochloric acid
IPTG	isopropyl- β-D-thiogalactopyranoside
LMW thiol	low molecular weight thiol
MRSA	methicillin-resistant *Staphylococcus aureus*
NaOCl	sodium hypochlorite
NEM	N-ethylmaleimide
OD_{500}	optical density at 500 nm
OxD	oxidation degree of the Brx-roGFP2 biosensor
roGFP2	redox-sensitive GFP2
ROS	reactive oxygen species
RSS	reactive sulfur species

Appendix A. Supplementary data

Supplementary data to this chapter can be found online at https://

doi.org/10.1016/j.freeradbiomed.2019.05.018.

References

[1] F.D. Lowy, *Staphylococcus aureus* infections, N. Engl. J. Med. 339 (8) (1998) 520–532.
[2] H.W. Boucher, G.R. Corey, Epidemiology of methicillin-resistant *Staphylococcus aureus*, Clin. Infect. Dis. 46 (Suppl 5) (2008) S344–S349.
[3] G.L. Archer, *Staphylococcus aureus*: a well-armed pathogen, Clin. Infect. Dis. 26 (5) (1998) 1179–1181.
[4] D.M. Livermore, Antibiotic resistance in staphylococci, Int. J. Antimicrob. Agents 16 (Suppl 1) (2000) S3–S10.
[5] J.N. Pendleton, S.P. Gorman, B.F. Gilmore, Clinical relevance of the ESKAPE pathogens, Expert Rev. Anti Infect. Ther. 11 (3) (2013) 297–308.
[6] R.S. Rivlin, Historical perspective on the use of garlic, J. Nutr. 131 (3s) (2001) 951S–954S.
[7] R.S. Rivlin, Is garlic alternative medicine? J. Nutr. 136 (3 Suppl) (2006) 713S–715S.
[8] A. Rabinkov, X.Z. Zhu, G. Grafi, G. Galili, D. Mirelman, Alliin lyase (Alliinase) from garlic (Allium sativum). Biochemical characterization and cDNA cloning, Appl. Biochem. Biotechnol. 48 (3) (1994) 149–171.
[9] A. Stoll, E. Seebeck, The specificity of the alliinase from *Allium sativum*, C. R. Hebd. Seances Acad. Sci. 232 (15) (1951) 1441–1442.
[10] J. Borlinghaus, F. Albrecht, M.C. Gruhlke, I.D. Nwachukwu, A.J. Slusarenko, Allicin: chemistry and biological properties, Molecules 19 (8) (2014) 12591–12618.
[11] U. Münchberg, A. Anwar, S. Mecklenburg, C. Jacob, Polysulfides as biologically active ingredients of garlic, Org. Biomol. Chem. 5 (10) (2007) 1505–1518.
[12] R. Tocmo, Y. Wu, D. Liang, V. Fogliano, D. Huang, Boiling enriches the linear polysulfides and the hydrogen sulfide-releasing activity of garlic, Food Chem. 221 (2017) 1867–1873.
[13] J. Reiter, N. Levina, M. van der Linden, M. Gruhlke, C. Martin, A.J. Slusarenko, Diallylthiosulfinate (Allicin), a volatile antimicrobial from garlic (*Allium sativum*), kills human lung pathogenic bacteria including MDR strains as a vapor, Molecules 22 (10) (2017).
[14] A. Müller, J. Eller, F. Albrecht, P. Prochnow, K. Kuhlmann, J.E. Bandow, A.J. Slusarenko, L.I. Leichert, Allicin induces thiol stress in bacteria through *S*-allylmercapto modification of protein cysteines, J. Biol. Chem. 291 (22) (2016) 11477–11490.
[15] A. Rabinkov, T. Miron, L. Konstantinovski, M. Wilchek, D. Mirelman, L. Weiner, The mode of action of allicin: trapping of radicals and interaction with thiol containing proteins, Biochim. Biophys. Acta 1379 (2) (1998) 233–244.
[16] M. Arbach, T.M. Santana, H. Moxham, R. Tinson, A. Anwar, M. Groom, C.J. Hamilton, Antimicrobial garlic-derived diallyl polysulfanes: interactions with biological thiols in *Bacillus subtilis*, Biochim. Biophys. Acta Gen. Subj. 1863 (6) (2019) 1050–1058.
[17] W.D. Minchin, A Study in Tubercule Virus Polymorphism, and the Treatment of Tuberculosis and Lupus with Oleum Allii, Bailliere, Tindall and Cox, London, UK, 1927.
[18] M.C.H. Gruhlke, H. Antelmann, J. Bernhardt, V. Kloubert, L. Rink, A.J. Slusarenko, The human allicin-proteome: *S*-thioallylation of proteins by the garlic defence substance allicin and its biological effects, Free Radic. Biol. Med. 131 (2019) 144–153.
[19] T. Miron, I. Listowsky, M. Wilchek, Reaction mechanisms of allicin and allyl-mixed disulfides with proteins and small thiol molecules, Eur. J. Med. Chem. 45 (5) (2010) 1912–1918.
[20] T. Miron, A. Rabinkov, D. Mirelman, M. Wilchek, L. Weiner, The mode of action of allicin: its ready permeability through phospholipid membranes may contribute to its biological activity, Biochim. Biophys. Acta 1463 (1) (2000) 20–30.
[21] M.C. Gruhlke, B. Hemmis, U. Noll, R. Wagner, H. Luhring, A.J. Slusarenko, The defense substance allicin from garlic permeabilizes membranes of *Beta vulgaris, Rhoeo discolor, Chara corallina* and artificial lipid bilayers, Biochim. Biophys. Acta 1850 (4) (2015) 602–611.
[22] J.G. Sheppard, T.E. Long, Allicin-inspired thiolated fluoroquinolones as antibacterials against ESKAPE pathogens, Bioorg. Med. Chem. Lett 26 (22) (2016) 5545–5549.
[23] J.G. Sheppard, J.P. McAleer, P. Saralkar, W.J. Geldenhuys, T.E. Long, Allicin-inspired pyridyl disulfides as antimicrobial agents for multidrug-resistant *Staphylococcus aureus*, Eur. J. Med. Chem. 143 (2018) 1185–1195.
[24] G.T.M. Getti, P.L. Poole, Allicin causes fragmentation of the peptidoglycan coat in *Staphylococcus aureus* by effecting synthesis and aiding hydrolysis: a determination by MALDI-TOF mass spectrometry on whole cells, J. Med. Microbiol. 68 (4) (2019) 667–677.
[25] G.L. Newton, R.C. Fahey, M. Rawat, Detoxification of toxins by bacillithiol in *Staphylococcus aureus*, Microbiology 158 (Pt 4) (2012) 1117–1126.
[26] D.C. Pöther, P. Gierok, M. Harms, J. Mostertz, F. Hochgräfe, H. Antelmann, C.J. Hamilton, I. Borovok, M. Lalk, Y. Aharonowitz, M. Hecker, Distribution and infection-related functions of bacillithiol in *Staphylococcus aureus*, Int. J. Med. Microbiol. 303 (3) (2013) 114–123.
[27] A.C. Posada, S.L. Kolar, R.G. Dusi, P. Francois, A.A. Roberts, C.J. Hamilton, G.Y. Liu, A. Cheung, Importance of bacillithiol in the oxidative stress response of *Staphylococcus aureus*, Infect. Immun. 82 (1) (2014) 316–332.
[28] P. Chandrangsu, V.V. Loi, H. Antelmann, J.D. Helmann, The role of bacillithiol in Gram-positive *Firmicutes*, Antioxidants Redox Signal. 28 (6) (2018) 445–462.
[29] B.K. Chi, K. Gronau, U. Mäder, B. Hessling, D. Becher, H. Antelmann, *S*-bacillithiolation protects against hypochlorite stress in *Bacillus subtilis* as revealed by transcriptomics and redox proteomics, Mol. Cell. Proteom. 10 (11) (2011) M111 009506.
[30] B.K. Chi, A.A. Roberts, T.T. Huyen, K. Bäsell, D. Becher, D. Albrecht, C.J. Hamilton, H. Antelmann, *S*-bacillithiolation protects conserved and essential proteins against hypochlorite stress in *Firmicutes* bacteria, Antioxidants Redox Signal. 18 (11) (2013) 1273–1295.
[31] M. Imber, N.T.T. Huyen, A.J. Pietrzyk-Brzezinska, V.V. Loi, M. Hillion, J. Bernhardt, L. Thärichen, K. Kolsek, M. Saleh, C.J. Hamilton, L. Adrian, F. Gräter, M.C. Wahl, H. Antelmann, Protein *S*-bacillithiolation functions in thiol protection and redox regulation of the glyceraldehyde-3-phosphate dehydrogenase Gap in *Staphylococcus aureus* under hypochlorite stress, Antioxidants Redox Signal. 28 (6) (2018) 410–430.
[32] P.R. Chen, T. Bae, W.A. Williams, E.M. Duguid, P.A. Rice, O. Schneewind, C. He, An oxidation-sensing mechanism is used by the global regulator MgrA in *Staphylococcus aureus*, Nat. Chem. Biol. 2 (11) (2006) 591–595.
[33] M. Hillion, H. Antelmann, Thiol-based redox switches in prokaryotes, Biol. Chem. 396 (5) (2015) 415–444.
[34] P.R. Chen, S. Nishida, C.B. Poor, A. Cheng, T. Bae, L. Kuechenmeister, P.M. Dunman, D. Missiakas, C. He, A new oxidative sensing and regulation pathway mediated by the MgrA homologue SarZ in *Staphylococcus aureus*, Mol. Microbiol. 71 (1) (2009) 198–211.
[35] P.R. Chen, P. Brugarolas, C. He, Redox signaling in human pathogens, Antioxidants Redox Signal. 14 (6) (2011) 1107–1118.
[36] M.J. Horsburgh, M.O. Clements, H. Crossley, E. Ingham, S.J. Foster, PerR controls oxidative stress resistance and iron storage proteins and is required for virulence in *Staphylococcus aureus*, Infect. Immun. 69 (6) (2001) 3744–3754.
[37] C.J. Ji, J.H. Kim, Y.B. Won, Y.E. Lee, T.W. Choi, S.Y. Ju, H. Youn, J.D. Helmann, J.W. Lee, *Staphylococcus aureus* PerR is a hypersensitive hydrogen peroxide sensor using iron-mediated histidine oxidation, J. Biol. Chem. 290 (33) (2015) 20374–20386.
[38] V.V. Loi, T. Busche, K. Tedin, J. Bernhardt, J. Wollenhaupt, N.T.T. Huyen, C. Weise, J. Kalinowski, M.C. Wahl, M. Fulde, H. Antelmann, Redox-sensing under hypochlorite stress and infection conditions by the Rrf2-family repressor HypR in *Staphylococcus aureus*, Antioxidants Redox Signal. 29 (7) (2018) 615–636.
[39] V. Van Loi, T. Busche, T. Preuss, J. Kalinowski, J. Bernhardt, H. Antelmann, The AGXX antimicrobial coating causes a thiol-specific oxidative stress response and protein *S*-bacillithiolation in *Staphylococcus aureus*, Front. Microbiol. 9 (2018).
[40] V.V. Loi, M. Harms, M. Müller, N.T.T. Huyen, C.J. Hamilton, F. Hochgräfe, J. Pane-Farre, H. Antelmann, Real-time imaging of the bacillithiol redox potential in the human pathogen *Staphylococcus aureus* using a genetically encoded bacilliredoxin-fused redox biosensor, Antioxidants Redox Signal. 26 (15) (2017) 835–848.
[41] N. Linzner, V.V. Loi, V.N. Fritsch, Q.N. Tung, S. Stenzel, M. Wirtz, R. Hell, C. Hamilton, K. Tedin, M. Fulde, H. Antelmann, *Staphylococcus aureus* uses the bacilliredoxin (BrxAB)/bacillithiol disulfide reductase (YpdA) redox pathway to defend against oxidative stress under infections, BioRxiv (2019), https://doi.org/10.1101/624676.
[42] M.C. Gruhlke, D. Portz, M. Stitz, A. Anwar, T. Schneider, C. Jacob, N.L. Schlaich, A.J. Slusarenko, Allicin disrupts the cell's electrochemical potential and induces apoptosis in yeast, Free Radic. Biol. Med. 49 (12) (2010) 1916–1924.
[43] J.A. Vizcaino, A. Csordas, N. Del-Toro, J.A. Dianes, J. Griss, I. Lavidas, G. Mayer, Y. Perez-Riverol, F. Reisinger, T. Ternent, Q.W. Xu, R. Wang, H. Hermjakob, Update of the PRIDE database and its related tools, Nucleic Acids Res. 44 (22) (2016) 11033.
[44] E.W. Deutsch, A. Csordas, Z. Sun, A. Jarnuczak, Y. Perez-Riverol, T. Ternent, D.S. Campbell, M. Bernal-Llinares, S. Okuda, S. Kawano, R.L. Moritz, J.J. Carver, M. Wang, Y. Ishihama, N. Bandeira, H. Hermjakob, J.A. Vizcaino, The ProteomeXchange consortium in 2017: supporting the cultural change in proteomics public data deposition, Nucleic Acids Res. 45 (D1) (2017) D1100–D1106.
[45] M.I. Love, W. Huber, S. Anders, Moderated estimation of fold change and dispersion for RNA-seq data with DESeq2, Genome Biol. 15 (12) (2014) 550.
[46] R. Hilker, K.B. Stadermann, O. Schwengers, E. Anisiforov, S. Jaenicke, B. Weisshaar, T. Zimmermann, A. Goesmann, ReadXplorer 2-detailed read mapping analysis and visualization from one single source, Bioinformatics 32 (24) (2016) 3702–3708.
[47] H. Mehlan, F. Schmidt, S. Weiss, J. Schuler, S. Fuchs, K. Riedel, J. Bernhardt, Data visualization in environmental proteomics, Proteomics 13 (18–19) (2013) 2805–2821.
[48] M. Wetzstein, U. Völker, J. Dedio, S. Löbau, U. Zuber, M. Schiesswohl, C. Herget, M. Hecker, W. Schumann, Cloning, sequencing, and molecular analysis of the *dnaK* locus from *Bacillus subtilis*, J. Bacteriol. 174 (10) (1992) 3300–3310.
[49] B.K. Chi, K. Kobayashi, D. Albrecht, M. Hecker, H. Antelmann, The paralogous MarR/DUF24-family repressors YodB and CatR control expression of the catechol dioxygenase CatE in *Bacillus subtilis*, J. Bacteriol. 192 (18) (2010) 4571–4581.
[50] A. Gaballa, G.L. Newton, H. Antelmann, D. Parsonage, H. Upton, M. Rawat, A. Claiborne, R.C. Fahey, J.D. Helmann, Biosynthesis and functions of bacillithiol, a major low-molecular-weight thiol in Bacilli, Proc. Natl. Acad. Sci. U. S. A. 107 (14) (2010) 6482–6486.
[51] T.T. Nguyen, W. Eiamphungporn, U. Mäder, M. Liebeke, M. Lalk, M. Hecker, J.D. Helmann, H. Antelmann, Genome-wide responses to carbonyl electrophiles in *Bacillus subtilis*: control of the thiol-dependent formaldehyde dehydrogenase AdhA and cysteine proteinase YraA by the MerR-family regulator YraB (AdhR), Mol. Microbiol. 71 (4) (2009) 876–894.
[52] C.T. Dooley, T.M. Dore, G.T. Hanson, W.C. Jackson, S.J. Remington, R.Y. Tsien, Imaging dynamic redox changes in mammalian cells with green fluorescent protein indicators, J. Biol. Chem. 279 (21) (2004) 22284–22293.
[53] M. Hillion, J. Bernhardt, T. Busche, M. Rossius, S. Maass, D. Becher, M. Rawat, M. Wirtz, R. Hell, C. Rückert, J. Kalinowski, H. Antelmann, Monitoring global protein thiol-oxidation and protein S-mycothiolation in *Mycobacterium smegmatis*

under hypochlorite stress, Sci. Rep. 7 (1) (2017) 1195.
[54] J.L. Luebke, R.J. Arnold, D.P. Giedroc, Selenite and tellurite form mixed seleno- and tellurotrisulfides with CstR from *Staphylococcus aureus*, Metall 5 (4) (2013) 335–342.
[55] J.L. Luebke, J. Shen, K.E. Bruce, T.E. Kehl-Fie, H. Peng, E.P. Skaar, D.P. Giedroc, The CsoR-like sulfurtransferase repressor (CstR) is a persulfide sensor in *Staphylococcus aureus*, Mol. Microbiol. 94 (6) (2014) 1343–1360.
[56] H. Peng, J. Shen, K.A. Edmonds, J.L. Luebke, A.K. Hickey, L.D. Palmer, F.J. Chang, K.A. Bruce, T.E. Kehl-Fie, E.P. Skaar, D.P. Giedroc, Sulfide homeostasis and nitroxyl intersect via formation of reactive sulfur species in *Staphylococcus aureus*, mSphere 2 (3) (2017).
[57] G.I. Giles, K.M. Tasker, C. Jacob, Hypothesis: the role of reactive sulfur species in oxidative stress, Free Radic. Biol. Med. 31 (10) (2001) 1279–1283.
[58] D. Frees, U. Gerth, H. Ingmer, Clp chaperones and proteases are central in stress survival, virulence and antibiotic resistance of *Staphylococcus aureus*, Int. J. Med. Microbiol. 304 (2) (2014) 142–149.
[59] D. Frees, K. Savijoki, P. Varmanen, H. Ingmer, Clp ATPases and ClpP proteolytic complexes regulate vital biological processes in low GC, Gram-positive bacteria, Mol. Microbiol. 63 (5) (2007) 1285–1295.
[60] M. Imber, V.V. Loi, S. Reznikov, V.N. Fritsch, A.J. Pietrzyk-Brzezinska, J. Prehn, C. Hamilton, M.C. Wahl, A.K. Bronowska, H. Antelmann, The aldehyde dehydrogenase AldA contributes to the hypochlorite defense and is redox-controlled by protein *S*-bacillithiolation in *Staphylococcus aureus*, Redox Biol. 15 (2018) 557–568.
[61] M. Imber, A.J. Pietrzyk-Brzezinska, H. Antelmann, Redox regulation by reversible protein *S*-thiolation in Gram-positive bacteria, Redox Biol. 20 (2018) 130–145.
[62] I.V. Mikheyeva, J.M. Thomas, S.L. Kolar, A.R. Corvaglia, N. Gaiotaa, S. Leo, P. Francois, G.Y. Liu, M. Rawat, A.L. Cheung, YpdA, a putative bacillithiol disulfide reductase, contributes to cellular redox homeostasis and virulence in *Staphylococcus aureus*, Mol. Microbiol. 111 (4) (2019) 1039–1056.
[63] K.A. Higgins, H. Peng, J.L. Luebke, F.M. Chang, D.P. Giedroc, Conformational analysis and chemical reactivity of the multidomain sulfurtransferase, *Staphylococcus aureus* CstA, Biochemistry 54 (14) (2015) 2385–2398.
[64] J. Shen, M.E. Keithly, R.N. Armstrong, K.A. Higgins, K.A. Edmonds, D.P. Giedroc, *Staphylococcus aureus* CstB is a novel multidomain persulfide dioxygenase-sulfurtransferase involved in hydrogen sulfide detoxification, Biochemistry 54 (29) (2015) 4542–4554.
[65] D. Frees, A. Chastanet, S. Qazi, K. Sorensen, P. Hill, T. Msadek, H. Ingmer, Clp ATPases are required for stress tolerance, intracellular replication and biofilm formation in *Staphylococcus aureus*, Mol. Microbiol. 54 (5) (2004) 1445–1462.
[66] D. Frees, S.N. Qazi, P.J. Hill, H. Ingmer, Alternative roles of ClpX and ClpP in *Staphylococcus aureus* stress tolerance and virulence, Mol. Microbiol. 48 (6) (2003) 1565–1578.
[67] T. Horn, W. Bettray, A.J. Slusarenko, M.C.H. Gruhlke, *S*-allylmercaptoglutathione is a substrate for glutathione reductase (E.C. 1.8.1.7) from yeast *Saccharomyces cerevisiae*, Antioxidants (Basel) 7 (7) (2018).
[68] C. Hwang, H.F. Lodish, A.J. Sinskey, Measurement of glutathione redox state in cytosol and secretory pathway of cultured cells, Methods Enzymol. 251 (1995) 212–221.
[69] K. Van Laer, C.J. Hamilton, J. Messens, Low-molecular-weight thiols in thiol-disulfide exchange, Antioxidants Redox Signal. 18 (13) (2013) 1642–1653.
[70] M.C.H. Gruhlke, I. Schlembach, R. Leontiev, A. Uebachs, P.U.G. Gollwitzer, A. Weiss, A. Delaunay, M. Toledano, A.J. Slusarenko, Yap1p, the central regulator of the *S. cerevisiae* oxidative stress response, is activated by allicin, a natural oxidant and defence substance of garlic, Free Radic. Biol. Med. 108 (2017) 793–802.